Published in final edited form as:
J Immunol. 2010 November 15; 185(10): 5845–5858. doi:10.4049/jimmunol.1001796.

Store-operated Ca^{2+} entry through ORAI1 is critical for T cell mediated autoimmunity and allograft rejection[1]

Christie-Ann McCarl[*,†,2], **Sara Khalil**[*,2], **Jian Ma**[*,2], **Masatsugu Oh-hora**[†,2,3], **Megumi Yamashita**[‡,2], **Jens Roether**[†,2], **Takumi Kawasaki**[*,4], **Amit Jairaman**[‡], **Yoshiteru Sasaki**[†,5], **Murali Prakriya**[‡], and **Stefan Feske**[*,†]

[*] Department of Pathology, New York University Langone Medical Center, NY, NY 10016, USA

[†] Immune Disease Institute and Harvard Medical School, Boston, MA 02115, USA

[‡] Department of Molecular Pharmacology and Biological Chemistry, Northwestern University, Feinberg School of Medicine, Chicago, IL 60611, USA

Abstract

ORAI1 is the pore forming subunit of the Ca^{2+} release activated Ca^{2+} (CRAC) channel, which is responsible for store-operated Ca^{2+} entry (SOCE) in lymphocytes. A role for ORAI1 in T cell function *in vivo* has been inferred from *in vitro* studies of T cells from human immunodeficient patients with mutations in *ORAI1* and *Orai1*$^{-/-}$ mice but a detailed analysis of T cell mediated immune responses *in vivo* in mice lacking functional ORAI1 has been missing. We therefore generated *Orai1* knock-in mice (*Orai1*$^{KI/KI}$) expressing a nonfunctional ORAI1-R93W protein. Homozygosity for the equivalent ORAI1-R91W mutation abolishes CRAC channel function in human T cells resulting in severe immunodeficiency. Homozygous *Orai1*$^{KI/KI}$ mice die neonatally but *Orai1*$^{KI/KI}$ fetal liver chimeric mice are viable and show normal lymphocyte development. T and B cells from *Orai1*$^{KI/KI}$ mice display severely impaired SOCE and CRAC channel function resulting in a strongly reduced expression of several key cytokines including IL-2, IL-4, IL-17, IFN-γ and TNF-α in $CD4^+$ and $CD8^+$ T cells. Cell mediated immune responses *in vivo* that depend on T_H1, T_H2 and T_H17 cell function were severely attenuated in ORAI1 deficient mice. *Orai1*$^{KI/KI}$ mice lacked detectable contact hypersensitivity responses and tolerated skin allografts significantly longer than wildtype mice. In addition, T cells from *Orai1*$^{KI/KI}$ mice failed to induce colitis in an adoptive transfer model of inflammatory bowel disease. These findings reaffirm the critical role of ORAI1 for T cell function and provide new insights into the *in vivo* functions of CRAC channels for T cell mediated immunity.

Introduction

Activation of T cells in response to T cell receptor stimulation requires Ca^{2+} influx which mediates important Ca^{2+} dependent signaling events (1). Arguably the most important Ca^{2+} influx pathway in T cells is store-operated Ca^{2+} entry, so named because it is activated by

[1]This work was funded by a March of Dimes Foundation grant to S.F. and NIH grants AI066128 to S.F., AI054636 to Klaus Rajewsky and NS057499 to M.P.

Address correspondence to: Stefan Feske, M.D., New York University, Langone Medical Center, Department of Pathology, 550 First Avenue, New York, NY 10016, USA, feskes01@nyumc.org, Phone: +1-212-263-9066; Fax: +1-212-263-8211.
[2]These authors contributed equally to this study.
[3]Present address: Department of Cell Signaling, Tokyo Medical and Dental University, Tokyo 113-8549, Japan.
[4]Present address: Laboratory of Host Defense, WPI Immunology Frontier Research Center, Osaka University, Japan.
[5]Present address: Laboratory for Stem Cell Biology, RIKEN Center for Developmental Biology, Kobe, Japan.

Conflict of interest. S.F. is a co-founder of Calcimedica Inc. and member of its scientific advisory board.

depletion of endoplasmic reticulum (ER) Ca^{2+} stores following activation of phospholipase C (PLC) γ1 and production of inositol 1,4,5-triphosphate (InsP3). InsP3 binds to and opens InsP3 receptor ion channels allowing Ca^{2+} to efflux from the ER. Ca^{2+} release results in a transient increase in the intracellular Ca^{2+} concentration $[Ca^{2+}]_i$ and activation of CRAC channels in the plasma membrane (2). The CRAC channel is the prototypical store-operated Ca^{2+} channel and possesses unique electrophysiological properties including high Ca^{2+} selectivity and a very low single-channel conductance (< 1 pS) (3). The CRAC channel is encoded by *ORAI1 (*or *CRACM1),* a tetraspanning plasmamembrane protein that is structurally unrelated to other ion channels and which serves as the pore forming subunit of the channel (2,4). ORAI1-CRAC channels are activated through direct physical interaction with the ER Ca^{2+} sensors stromal interaction molecule (STIM) 1 and 2, transmembrane proteins located in the membrane of the ER (5).

CRAC channel activation and the resulting SOCE are required for various T cell functions including cytokine gene expression *in vitro* (1,6,7). In humans, the importance of ORAI1 and STIM1 *in vivo* is illustrated by a rare group of immunodeficiency diseases affecting patients with mutations in *ORAI1* and *STIM1* that abolish SOCE in T cells and other cell types (8–11). Whereas some mutations abolish ORAI1 or STIM1 protein expression, a missense mutation in ORAI1 results in a single amino acid substitution (R91W) located at the interface of the cytoplasmic N terminus with the first transmembrane domain of ORAI1. The mutant ORAI1-R91W protein is expressed but its CRAC channel function is abolished(12,13). Clinically, all ORAI1 and STIM1 deficient patients suffer from immunodeficiency with an increased susceptibility to infections. The latter has been attributed to defects in the activation of the patients' T cells from *in vitro* studies (14). In addition, non-immunological symptoms such as congenital muscular hypotonia and anhydrotic ectodermal dysplasia (EDA) are present in ORAI1 and STIM1 deficient patients but are not life threatening (10,11).

Mice lacking *Orai1* expression have been generated and, in contrast to human patients, die neonatally even under specific pathogen free conditions (15–18). A minority of surviving mice was severely runted indicating that ORAI1 serves critical functions outside the immune system. Hematopoietic lineage cells such as T and B cells (16), mast cells (17) and platelets (15) isolated from surviving $Orai1^{-/-}$ mice showed a defect in SOCE and impaired cell function. In one study(17), however, SOCE in ORAI1 deficient T cells was normal and T cell function only modestly impaired raising questions about the precise contribution of ORAI1 to SOCE in murine T cells. Because naive T cells also express ORAI2 and ORAI3, two highly conserved paralogues of ORAI1 (16,17), it was suggested that these molecules, especially ORAI2, could be responsible for the residual SOCE observed in ORAI1 deficient T cells (17). It is noteworthy that both ORAI2 and ORAI3 – when overexpressed together with STIM1 – are able to form functional Ca^{2+} channels with properties similar to those of the native CRAC channel (26,27), but the contribution of endogenously expressed ORAI2 and ORAI3 to SOCE and CRAC channel function has yet to be established.

Given the controversial role of ORAI1 for SOCE in naive T cells and B cell function, and because a systematic analysis of ORAI1 dependent, T cell mediated immune responses *in vivo* has been lacking, we generated *Orai1 knock-in* ($Orai1^{KI/KI}$) mice expressing a mutant ORAI1-R93W protein that is equivalent to the non-functional ORAI1-R91W mutant found in human SCID patients (12,18). $Orai1^{KI/KI}$ mice die neonatally, but fetal liver chimeric mice that homozygously express ORAI1-R93W in hematopoietic cells develop normally. T cells from chimeric $Orai1^{KI/KI}$ mice have a profound defect in SOCE and CRAC channel function that results in severely compromised T cell function *in vitro* and *in vivo.* $Orai1^{KI/KI}$ mice expressing a non-functional ORAI1 channel protein provide a useful tool to study the

role of ORAI1 for immune responses *in vivo*, and their phenotype can be directly compared to that of *Orai1*$^{-/-}$ mice and patients homozygous for the ORAI1-R91W mutation.

MATERIALS AND METHODS

Generation of *Orai1* knock-in mice (*Orai1*$^{KI/KI}$)

Gene targeting of the *Orai1 g*ene was performed by homologous recombination in B6/3 ES cells derived from C57BL/6 mice (TaconicArtemis GmbH, Koln, Germany) as described (18). Briefly, *Orai1*$^{KI/KI}$ mice were generated by replacing codon 93 (CGG encoding R93) in exon 1 of the *Orai1* gene with TGG (encoding W93). Chimeric mice with targeted *Orai1* alleles were generated by blastocyst injection of heterozygous *Orai1*$^{neo/+}$ ES cell clones, the Neo cassette was deleted by Cre expression under the control of the testis specific ACE promoter during spermatogenesis and founder *Orai1*$^{neo/+}$ chimeric mice were bred to C57BL/6 mice to establish *Orai1*$^{+/KI}$ mice. Successful gene-targeting was confirmed by two PCR approaches, detecting (1) the remaining loxP site in the *Orai1* locus after excision of the Neo^{r}/ACE-Cre cassette and (2) the mutated codon 93, which creates a recognition site for the restriction endonuclease PvuII (CAGCTG). Primers used for detection of the loxP site were: Forward 5′ATTTCCCAATACGTTCCACCTCCC; Reverse 5′ TCGTACCACCTTCTTGGGACTTGA. Primers used for PCR amplification of *Orai1* exon 1 (followed by PvuII digest) were: Forward 5′-TGGATCGGCCAGAGTTACTCC; Reverse 5′ GATTACATGCAGGGCAGACTTCTTA. *Stim1*$^{fl/fl}$ *Cd4-Cre* mice were generated as described (20).

Fetal liver chimeras and outbred mice

To generate fetal liver chimeras, fetal liver cells were obtained from E14.5 mouse embryos derived from matings of Orai1$^{KI/+}$ mice on the C57BL/6 background. *Orai1*$^{KI/KI}$ and *Orai1*$^{+/+}$ littermate control cells were injected intravenously into sublethally irradiated (4.5 + 4.5 Gy) *Rag2*$^{-/-}$, *cγ* $^{-/-}$ mice (Taconic) or *Rag2*$^{-/-}$ mice (Taconic). Reconstituted mice were sacrificed 5 – 6 weeks after transplantation to harvest blood, spleen, lymph nodes and thymus for isolation of lymphocytes. To generate homozygous *Orai1*$^{KI/KI}$ mice on a mixed genetic background, heterozygous *Orai1*$^{KI/+}$ mice on the C57BL/6 background were mated for 3–4 generations with mice of the outbred ICR strain (Taconic), after which *Orai1*$^{KI/+}$ mice were intercrossed to generate *Orai1*$^{KI/KI}$ N3f1 and *Orai1*$^{KI/KI}$ N4f1 mice, respectively. All mice were maintained in specific pathogen-free barrier facilities at Harvard Medical School and NYU Langone Medical Center and were used in accordance with protocols approved by the Institutional Animal Care and Use Committee (IACUC) at both institutions.

T cell isolation, differentiation and cell culture

CD4^{+} and CD8^{+} T cells and B220^{+} B cells were isolated from thymus, spleen and lymph nodes of *Orai1*$^{KI/KI}$ and *Orai1*$^{+/+}$control fetal liver chimeric mice by magnetic bead separation (Dynal) according to the manufacturers instructions. CD4^{+} and CD8^{+} T cells were differentiated into T_HN, T_H1 and cytotoxic T cells (CTL) by stimulation with plate-bound anti-CD3 and anti-CD28 antibodies for 2 days, followed by culture in DMEM medium containing either 20 U/ml IL-2 alone (T_HN, non-polarizing conditions), or 20 U/ml IL-2 plus IL-12 and anti-IL-4 (T_H1 conditions), or 100 U/ml IL-2 (CTL) for an additional 4 days. HEK293 cells were cultured in DMEM (Mediatech, Manassas, VA) at 37°C, 10% CO_2.

Quantitative realtime PCR

Total RNA was extracted from T cells, skeletal muscle and colon using Trizol reagent (Invitrogen, Carlsbad, CA). cDNA was synthesized from total RNA using oligo dT primers

and the Superscript II™ First-Strand kit (Invitrogen). Realtime PCR was performed using an iCycler system (BioRad, Hercules, CA) and SYBR Green dye (Applied Biosystems, Foster City, CA) with the following primer pairs: Orai1 (NM_175423): 5′ CCAAGCTCAAAGCTTCCAGC, 3′ GGTTGCTCATCGTCTTTAGTGC; Orai2 (NM_178751): 5′ TCCTCAGACACACCAAGG, 3′ GCAGAACATGATTGGTGTCTTTTG; Orai3 (NM_198424): 5′ GGATCCTGGGTTAAATGAGAG, 3′ GTCTGCACAACTGTCCTCAA; Ppia (AK028210): 5′ AGCTCTGAGCACTGGAGAGA, 3′ TAAAGCATACAGGTCCTTGGC; Gadp (BC083080.1): Forward: 5′CTGGAGAAACCTGCCAAGTA, reverse: 5′TGTTGCTGTAGCCGTATTCA; Atf3 (NM_007498): 5′ CCAGGTCTCTGCCTCAGAAG, 3′ CATCTCCAGGGGTCTGTTGT; Ddit3 (CHOP10, NM_007837): 5′ CATACACCACCACACCTGAAAG, 3′ CCGTTTCCTAGTTCTTCCTTGC; Bip (NM_022310): 5′ GAAAGGATGGTTAATGATGCTGAG, 3′ GTCTTCAATGTCCGCATCCTG; Il-17a (NM_010552.3): 5′ CTCCAGAAGGCCCTCAGACTAC, 3′ CTGTGTCAATGCGGAGGGAAAGCT; Ifng (NM_008337.3) 5′ GATGCATTCATGAGTATTGCCAAGT, 3′ GAGCTCATCCGAGTGGTCCAC. SYBR green signals were captured at the end of each polymerization step (72°C), a threshold was set in the linear part of the amplification curve and threshold cycles (C_T) for genes of interest were normalized to the C_T for Ppia (Fig. 4D) and Gadp (Fig. 6H, Supplemental Fig. 2C) house keeping gene control obtaining ΔC_T. Expression data were plotted as $0.5^{\Delta Ct}$ or percent of Gapd expression. The specificity of PCR amplification was verified by melt curve analysis and agarose gel electrophoresis of PCR products. The efficiency of PCR amplification was tested by serial dilutions and analyzed using iCycler software. mOrai1: 112.7 ± 12.1 % (n=6 repeat experiments); mOrai2: 96.7 ± 8.0 % (n=6); mOrai3: 121.4 ± 10.5 % (n=6); Ppia 93.3 ± 4.2 % (n=6).

Antibodies and flow cytometry

For flow cytometry, single-cell suspensions prepared from thymi, lymph nodes and spleens of *Orai1*$^{KI/KI}$ and *Orai1*$^{+/+}$ control mice were pre-incubated with anti-CD16/32 antibody (clone 93, eBioscience) followed by incubation with the following antibodies (all from eBioscience, San Diego, CA): anti-B220 (clone RA3-6B2), anti-CD-4 (clone GK1.5), anti-CD8 (clone 53-6.7), anti-CD25 (clone PC61.5), anti-CD44 (clone IM7), anti-TCRβ (clone H57-597), anti-CD69 (clone H1.2F3), anti-AA4.1 (clone AA4.1), anti-IgD (clone 11-26), anti-IL-2 (clone JES6-5H4), anti-IFN-γ (clone XMG1.2), anti-IL-4 (clone 11B11), anti-IL-10 (clone JES5-16E3), anti-granzyme B (clone 16G6), anti-Foxp3 (clone NRRF-30); anti-IgM (clone R6-60.2) antibody was purchased from BD Biosciences (San Jose, CA). For intracellular cytokine staining, T_HN cells or CTL were restimulated with 10 nM phorbol 12-myristate 13-acetate (PMA; Sigma) and 1 μM ionomycin (Sigma) for 6 h in the presence or absence of 2 μM cyclosporin A (EMD Biosciences). 5 μM brefeldin A was added during the last 2 h of stimulation. At the end of the stimulation, cells were incubated with anti-CD16/32 for 20 min on ice to block Fc receptors followed by incubation with antibodies to surface proteins for 20 min on ice. Cells were washed in FACS buffer (1% BSA in 1x PBS), fixed with 4% paraformaldehyde, and incubated with cytokine antibodies in permeabilization buffer (0.5% saponin in 1xPBS and 1% BSA). Fluorescence was measured using a LSRII flow cytometer and data were analyzed with FlowJo software (Treestar).

Proliferation assay

$CD4^+$ and $CD8^+$ T cells isolated from lymph nodes and spleen of *Orai1*$^{KI/KI}$ and *Orai1*$^{+/+}$control mice were loaded with 4 μM CarboxyFluoroscein Succinimidyl Ester (CFSE) directly following magnetic bead separation and stimulated with plate-bound anti-CD3 and anti-CD28 for 72 hours. Alternatively, cells were first differentiated into T_HN cells

(see above) for 3 days, then loaded with CFSE on day 3 and stimulated with anti-CD3 and anti-CD28 for 72 hours. Cells were stimulated for proliferation assays in the absence of exogenous IL-2. The number of cell divisions was analyzed using an LSRII flow cytometer.

In vitro T_{reg} suppression assay

T_{reg} mediated suppression was analyzed as described (20). Briefly, $CD4^+$ $CD25^+$ T cells were isolated from peripheral lymph nodes and spleen of wildtype and *Orai1*$^{KI/KI}$ chimeric mice by cell sorting using an iCyt Reflection parallel cell sorter (iCyt, Champaign, IL). $CD4^+$ $CD25^-$ T cells were isolated from peripheral lymph nodes by negative selection using CD25 MACS MicroBead Kit (Miltenyi Biotec) followed by labeling with 2 μM CFSE (Invitrogen) at 37°C for 3 min according to the manufacturer's instructions. $CD4^+$ $CD25^-$ T cells were stimulated with 0.3 μg/ml anti-CD3 (2C11) in the presence of 5 x 10^4 T cell depleted splenocytes (pre-treated with 40 mg/ml mitomycin C (Sigma) at 37°C for 30 min) and co-cultured with $CD4^+$ $CD25^+$ T_{reg} cells at various ratios for 72 hrs at 37°C in 96 well round bottom plates.

Allogenic skin transplantation

Tail-skin grafts from BALB/c mice (H-2^d) were harvested and transplanted onto the back of *Orai1*$^{KI/KI}$ and *Orai1*$^{+/+}$control fetal liver chimeric mice (C57BL/6 background, H-2^b). Donor skin from the base of the tail of BALB/c mice was removed and cut to the size of 8x8 mm for each skin graft. The hair on the left side of the thorax of the recipient mice was shaved and the epidermal and dermal layers of the skin removed to expose the underlying panniculus carnosus creating a graft bed of ~ 9x9 mm, slightly bigger than the size of skin graft. Skin allografts were fixed on graft-beds with nylon black monofilament (6-0, Tyco Healthcare, Norwalk, CT, USA) at the corners. Recipients of skin allograft transplants were monitored daily for size and integrity of the skin graft. The graft was considered rejected, when the size was < 20% of the original transplanted skin.

Contact hypersensitivity

Orai1$^{KI/KI}$ and *Orai1*$^{+/+}$control mice were sensitized to hapten 5–6 weeks after transfer of fetal liver cells by epicutaneous application of 200 μl 0.5% FITC (Sigma) diluted 1:1 in acetone/dibuthyl pthalate (vehicle) onto the shaved abdomen or left unsensitized. 6 days later, baseline thickness of both ears was measured with a dial thickness gauge (GWJ Co., Hacienda Heights, CA). Each side of the right and left ear was then treated with 10 μL of 0.5% FITC (dissolved in acetone/dibuthyl pthalate) and vehicle alone, respectively. Thickness of both ears was measured 24 hours later in sensitized and non-sensitized animals. The change in ear thickness (ΔT) was calculated as ΔT = [ear thickness 24 h after elicitation] – [baseline ear thickness] as described (21).

Adoptive transfer colitis

$CD4^+$ $CD25^-$ $CD45RB^{hi}$ T cells were isolated from peripheral lymph nodes and spleen of wildtype and *Orai1*$^{KI/KI}$ chimeric mice by staining with anti-CD4 (clone GK1.5), anti-CD25 (clone PC61.5) and anti-CD45RB (clone C363.16A, all from eBioscience) antibodies and cell sorting using an iCyt Reflection parallel cell sorter (iCyt, Champaign, IL). > 95% purity of the sorted $CD4^+CD25^-CD45RB^{hi}$ T cells was confirmed by flow cytometry using a LSRII (BD Biosciences) and 5 x 10^5 cells were injected i.p. into 3 – 4 months old syngeneic *Rag2*$^{-/-}$ mice. Recipient mice were weighed and assessed for disease symptoms weekly. Mice were sacrificed and organs harvested 12 weeks after adoptive cell transfer.

Isolation of Colon and Histology

Colons of mice were excised and flushed with PBS, cut longitudinally and rolled as described (22). For histology, proximal and distal colon sections were fixed in 4% paraformaldehyde, paraffin-embedded and stained with hematoxylin and eosin using standard protocols. Colon histology was scored in a blinded fashion by two individuals using a grading system from 0–5 as described (23). 0, no changes; 1, minimal scattered mucosal inflammatory cell infiltrates, with or without epithelial hyperplasia; 2, mild scattered to diffuse inflammatory cell infiltrates, sometimes extending into the submucosa and associated with erosions, with minimal to mild epithelial hyperplasia and minimal to mild mucin depletion from goblet cells; 3, mild to moderate inflammatory cell infiltrates that were sometimes transmural, often associated with ulceration, with moderate epithelial hyperplasia and mucin depletion; 4, marked inflammatory cell infiltrates that were often transmural and associated with ulceration, with marked epithelial hyperplasia and mucin depletion; 5, marked transmural inflammation with severe ulceration and loss of intestinal glands.

Cytokine ELISA

Cytokine levels were measured in cell culture supernatants of cells isolated from mesenteric lymph nodes and spleens that were stimulated for 48 hours with plate-bound anti-CD3ε antibody (5 μg/ml). Supernatants were harvested, centrifuged to remove cell debris, and stored at −20ºC. IL-17A, IFN-γ, and TNF-α were detected in triplicate measurements by Ready-SET-Go ELISA kits (eBioscience) following the manufacturer's instructions. Absorbance was measured on a DTX880 Multimode Detector (Beckman Coulter).

Calcium measurements

$CD4^+$ T, $CD8^+$ T and $CD19^+$ B cells were isolated from lymphnodes of *Orai1*$^{KI/KI}$ and littermate control mice and either used for calcium measurements directly or differentiated *in vitro* for 6 days (see above). For time-lapse Ca^{2+} imaging, cells were loaded with 1 μM fura-2/AM (Invitrogen) for 30 min at 22–25ºC at a concentration of $1x10^6$ cells/ml and attached to poly-L-lysine-coated coverslips for 15 min. T cells were stimulated by passive store depletion with 1 μM thapsigargin or anti-CD3 crosslinking by incubating cells with 5 μg/ml biotin-conjugated anti-CD3 mAb (clone 2C11, Invitrogen) for 15 min at 22–25ºC followed by perfusion with 10 μg/ml streptavidin (Pierce). B cells were stimulated with 1 μM thapsigargin. Measurements of $[Ca^{2+}]_i$ were conducted at 22–25ºC using a Zeiss Axiovert S200 epifluorescence microscope and OpenLab imaging software (Improvision) as described (13). ~ 100 cells per experiment were analyzed using Igor Pro analysis software (Wavemetrics, Lake Oswego, OR). For calcium measurements by flow cytometry, cells isolated from lymph nodes of *Orai1*$^{KI/KI}$ and littermate control mice were simultaneously incubated with 1 μM Fluo-4/AM (Invitrogen) and antibodies to CD4, CD44 and CD62L for 15 min at 22–25ºC. Cells were stimulated with 1 μM thapsigargin and calcium levels analyzed on a LSRII flow cytometer (Becton Dickinson). Data were analyzed using FlowJo software (Tree Star).

Fluorescence resonance energy transfer (FRET)

FRET experiments were conducted and analyzed as described previously (24). Briefly, HEK293 cells were transfected with fusion proteins of wildtype Orai1–CFP (cyan fluorescent protein) and wildtype Orai1–YFP (yellow fluorescent protein) or wildtype Orai1–CFP and R91W-ORAI1-YFP. FRET was measured in non-stimulated cells in 2 mM extracellular Ca^{2+} followed by stimulation with 1 μM thapsigargin in 0 mM extracellular Ca^{2+}.

Transmission Electron Microscopy

Sacrificed mice were fixed by cardiac perfusion with 4% paraformaldehyde / 1% glutaraldehyde in 0.1 M sodium phosphate buffer, pH 7.3. After dissection, fixation was allowed to continue at room temperature for 90 min or 4°C overnight. Cardiac and skeletal muscle tissue was washed with 100 mM Tris (pH 7.2) and 160 mM sucrose for 30 minutes followed by washes in isoosmotic phosphate buffer (150 mM sodium chloride, 5 mM potassium chloride, 10 mM sodium phosphate, pH 7.3) for 30 min twice. Following treatment with 1% osmium tetroxide in 140 mM sodium phosphate (pH 7.3) for 1h, muscle tissue was washed (twice for 1h) in water. The muscle was stained en bloc with saturated uranyl acetate for 1h, dehydrated in ethanol and embedded in Epon (Electron Microscopy Sciences, Hatfield, PA). Semi-thin sections were cut at 1 mm and stained with 1% Toluidine Blue to evaluate the quality of preservation. Ultrathin sections (60 nm) were cut and stained with uranyl acetate and lead citrate by standard methods. Stained grids were examined using a Philips CM-12 electron microscope (FEI; Eindhoven, The Netherlands) and photographed with a Gatan Erlangshen ES1000W digital camera (Model 785, 4k x2.7k; Gatan, Inc., Pleasanton, CA).

Patch-clamp measurements

$CD4^+$ T cells were cultured in T_HN conditions and harvested at days 5–6. Patch-clamp recordings were performed using an Axopatch 200 amplifier (Axon Instruments, Foster City, CA) interfaced to an ITC-18 input/output board (Instrutech, Port Washington, NY) and an iMac G5 computer. Currents were filtered at 1 kHz with a 4-pole Bessel filter and sampled at 5 kHz. Recording electrodes were pulled from 100-μl pipettes, coated with Sylgard, and fire-polished to a final resistance of 2–5 MΩ. Stimulation and data acquisition and analysis were performed using in-house routines developed on the Igor Pro platform (Wavemetrics, Lake Oswego, OR). All data were corrected for the liquid junction potential of the pipette solution relative to Ringer's in the bath (−10 mV) and for leak currents collected in 20 mM $[Ca^{2+}]_o$ + 25 μM La^{3+}. The standard extracellular Ringer solution contained (in mM): 130 NaCl, 4.5 KCl, 20 $CaCl_2$, 1 $MgCl_2$, 10 D-glucose, and 5 Na-Hepes (pH 7.4). The standard divalent-free (DVF) Ringer solutions contained (in mM): 150 NaCl, 10 HEDTA, 1 EDTA and 10 Hepes (pH 7.4). 25 nM charybdotoxin (Sigma) was added to all extracellular solutions to eliminate contamination from Kv1.3 channels. The standard internal solution contained (in mM): 145 Cs aspartate, 8 mM $MgCl_2$, 10 BAPTA, and 10 Cs-Hepes (pH 7.2). Averaged results are presented as the mean value ± s.e.m.

Statistical Analysis

Unless indicated otherwise, the unpaired, two-tailed Student's *t* test was used for all statistical analyses. Differences were considered significant when *p* values were at least <0.05. The logrank test was used to compare the survival of skin allografts in Fig. 5.

Results

Perinatal lethality in "knock-in" mice homozygous for Orai1-R93W mutation

Orai1$^{KI/KI}$ mice were generated by replacing exon 1 of the *Orai1* gene by homologous recombination with a mutant allele carrying a C>T missense mutation resulting in an R→W single amino acid substitution at position 93 (Supplemental Fig. 1)(18). Mice heterozygous for the Orai1-R93W mutation (*Orai1*$^{KI/+}$) developed normally on a C57BL/6 background with survival rates comparable to wildtype littermate controls (Fig. 1A). By contrast, the numbers of homozygous *Orai1*$^{KI/KI}$ mice were reduced in late gestation at E18.5 (Fig. 1B) and at birth relative to the expected Mendelian distribution and died within 12 hours post partum (Fig. 1A). At birth, *Orai1*$^{KI/KI}$ pups were of normal size, motile and lacked obvious

signs of paralysis or hypoxemia during the first hours post partum. Survival of <30% of *Orai1*$^{KI/KI}$ pups could be rescued for up to 9 days by crossing *Orai1*$^{KI/+}$ mice to the outbred ICR strain for 3–4 generations followed by intercrossing of heterozygotes (Fig. 1A). Nevertheless, the majority of *Orai1*$^{KI/KI}$ mice on this background died on the day of birth, all remaining mice died within 9 days. Newborn *Orai1*$^{KI/KI}$ pups lacked visible milk patches (Supplemental Fig. 2A) and showed signs of severe dehydration. The few mice that survived until days 5–9 after birth were severely runted. The poor survival of *Orai1*$^{KI/KI}$ pups is in contrast to a ~ 50% survival rate of *Orai1*$^{-/-}$ mice on an ICR background (16) and greater survival of Orai1 deficient mice generated by insertional mutagenesis on a mixed genetic background (15, 17).

Orai1$^{KI/KI}$ embryos (E16.5) and newborn pups lacked gross morphological abnormalities that could account for the perinatal lethality (not shown). In particular, no histological abnormalities in skeletal muscle fibers from leg, intercostal and diaphragm muscles were detected. This is in contrast to atrophic type II muscle fibers in an ORAI1-R91W mutant patient suffering from congenital myopathy (10) and *Stim1*$^{-/-}$ mice, which showed a marked reduction in muscle cross-sectional area compared to wildtype mice. Ultrastructural analysis by EM revealed largely intact myofibril structure and cell organelles in skeletal muscle from *Orai1*$^{KI/KI}$ mice (Fig. 1C–D). A small fraction (< 5%) of skeletal myofibers, however, showed markedly swollen mitochondria with abnormal cristae structure (Fig. 1E). Comparable morphological abnormalities were absent in skeletal muscle samples from wildtype littermate controls (not shown). The mitchondrial changes in *Orai1*$^{KI/KI}$ mice, which were also observed in cardiomyocytes (Supplemental Fig. 2B), are reminiscent of a similar, although more pronounced, mitochondriopathy in *Stim1*-deficient mice which have been suggested to die perinatally from a skeletal myopathy (25). In addition, we observed dilated ER structures and nuclear envelopes in a small minority (< 5%) of cells present in skeletal muscles of *Orai1*$^{KI/KI}$ mice suggestive of ER stress. mRNA levels of ER stress associated genes, however, were not increased in muscle from *Orai1*$^{KI/KI}$ compared to wildtype mice (Supplemental Fig. 2C). Taken together, *Orai1*$^{KI/KI}$ mice show severely impaired perinatal survival indicative of an important role for ORAI1 in tissues outside the immune system despite the lack of overt signs of myopathy in *Orai1*$^{KI/KI}$ mice.

Severe defect in SOCE and CRAC channel currents in T cells from *Orai1*$^{KI/KI}$ mice

To study the role of ORAI1 for lymphocyte development and immune responses *in vivo*, we generated fetal liver chimeric mice by transferring stem cells harvested from the liver of *Orai1*$^{KI/KI}$ or *Orai1*$^{+/+}$ embryos on day E14.5 into sub-lethally irradiated *Rag2*$^{-/-}$ or *Rag2*$^{-/-}$ *cγ* $^{-/-}$ C57BL/6 mice. *Orai1*$^{KI/KI}$ fetal liver chimeras (FLC) were viable and their T cells, isolated 5 to 8 weeks after stem cell transfer, were homozygous for the targeted *Orai1* locus (Fig. 1F). Lymphocyte numbers in the spleen and lymph nodes, including those of T, B, NK, NKT and dendritic cells, were comparable in *Orai1*$^{KI/KI}$ and *Orai1*$^{+/+}$ control mice (Fig. 1G). This finding suggested that overall lymphocyte development is normal, enabling us to analyze T cell function in *Orai1*$^{KI/KI}$ mice.

Human patients homozygous for the ORAI1-R91W mutation or mutations that abolish ORAI1 expression lack CRAC channel function and SOCE in T cells (8–10,12). In mice, the role of ORAI1 for CRAC channel function in T cells has been debated as SOCE is impaired in T cells from *Orai1*$^{-/-}$ mice (16), whereas T cells from another strain of *Orai1* deficient mice have normal Ca^{2+} influx (17). To investigate the role of ORAI1 for SOCE in mouse T cells further, we analyzed Ca^{2+} influx in *Orai1*$^{KI/KI}$ T cells at varying stages of differentiation. SOCE was measured in $CD4^+$ T cells from *Orai1*$^{KI/KI}$ mice that were cultured *in vitro* under non-polarizing (T_HN) or T_H1 polarizing conditions and $CD8^+$ T cells differentiated *in vitro* into cytotoxic T cells. Ca^{2+} influx in response to passive store depletion with the sarco/endoplasmic reticulum Ca^{2+} ATPase (SERCA) inhibitor

thapsigargin was severely compromised in $CD4^+$ T_H1 and T_HN cells and $CD8^+$ T cells apparent in strongly reduced peak Ca^{2+} levels and initial rates of Ca^{2+} influx (Fig. 2A–C;Supplemental Fig. 3A–C). This finding is consistent with the complete lack of SOCE in T cell lines from human patients homozygous for the ORAI1-R91W mutation, although in contrast to patient T cells a very small residual Ca^{2+} influx was observed in mouse T_H1, T_HN and $CD8^+$ T cells (13).

The small residual Ca^{2+} influx observed in T cells from *Orai1*$^{KI/KI}$ mice could be due to vestigial function of the mutant ORAI1^{R93W} protein or, alternatively, another Ca^{2+} channel with properties distinct from ORAI1 CRAC channels such as transient receptor potential (TRP) or other non-selective cation channels. To test these hypotheses, we analyzed CRAC channel currents in $CD4^+$ T cells from *Orai1*$^{KI/KI}$ mice differentiated into T_HN cells *in vitro*. A small residual CRAC channel current was observed in *Orai1*$^{KI/KI}$ T cells following passive store depletion with thapsigargin in the presence of either 20 mM extracellular Ca^{2+} ($Ca^{2+}{}_o$) or a Na^+-containing divalent free (DVF) solution. I_{CRAC} amplitudes in *Orai1*$^{KI/KI}$ T cells were ~ 15% (20 mM Ca^{2+}) and 13% (DVF) of those in control T cells (Fig. 2D–F). The electrophysiological properties of the residual current in T cells from *Orai1*$^{KI/KI}$ mice were indistinguishable from I_{CRAC} in T cells from littermates controls or human T cells (13) in the following respects: (i) block of Ca^{2+} current by La^{3+} (Fig. 2D, E, left panels); (ii) depotentiation of Na^+ current in divalent-free (DVF) solution over tens of seconds (Supplemental Fig. 4); (iii) block of Na^+ current by micromolar concentrations of Ca^{2+} (not shown) and (iv) fast inactivation of Ca^{2+} current (not shown). Taken together, these data show that the weak Ca^{2+} current and SOCE in T cells from *Orai1*$^{KI/KI}$ mice are due to a calcium channel with properties indistinguishable from I_{CRAC}. Vestigial function of the mutant ORAI1^{R93W} protein, however, is unlikely because a residual Ca^{2+} current of comparable magnitude had been observed in T cells from *Orai1*$^{-/-}$ mice (16) and because T cells from human patients homozygous for the ORAI1-R91W mutation had no recordable I_{CRAC} (12, 13). Instead, residual Ca^{2+} currents in *Orai1*$^{KI/KI}$ T cells may result from another SOC channel, for instance ORAI2 or ORAI3. Residual Ca^{2+} currents in *Orai1*$^{KI/KI}$ T cells did not, however, show any of the hallmarks reported for ORAI2 and ORAI3 – when these molecules were overexpressed together with STIM1 – such as potentiation by 50 μM 2-APB or Ca^{2+} dependent reactivation (not shown) (26, 27). Taken together, our data show that ORAI1 is critical for CRAC channel function in differentiated mouse T cells and accounts for the majority of store-operated Ca^{2+} influx.

Impaired SOCE with residual Ca^{2+} influx in T cells isolated from *Orai1*$^{KI/KI}$ mice

ORAI2, but not ORAI1, was suggested to be responsible for SOCE in naive T cells because naive T cells from one ORAI1 deficient mouse strain had normal SOCE and expressed very high levels of ORAI2 mRNA compared to those of ORAI1 and ORAI3 (17). These findings are in contrast to reduced SOCE in CRAC currents in naive T cells of another *Orai1*$^{-/-}$ strain (16). To analyze the role of ORAI1 in naive T and B cells, we measured SOCE in $CD4^+$ and $CD8^+$ T cells and $B220^+$ B cells freshly isolated from *Orai1*$^{KI/KI}$ mice. We observed an almost complete defect in Ca^{2+} influx in splenic $B220^+$ B cells from *Orai1*$^{KI/KI}$ mice following thapsigargin stimulation (Fig. 3A) consistent with similar findings in B cells from *Orai1*$^{-/-}$ *mice* (16). Importantly, a pronounced – albeit incomplete – defect in SOCE was observed in naïve $CD4^+$ and $CD8^+$ T cells from *Orai1*$^{KI/KI}$ mice which is apparent in both reduced peak Ca^{2+} levels as well as attenuated rates of Ca^{2+} influx (the latter being an indirect read-out for Ca^{2+} channel activity) (Fig. 3B–D). This finding indicates that ORAI1 is required for CRAC channel function and SOCE in naive T cells. It is of note that the SOCE defect in naive $CD4^+$ and $CD8^+$ T cells from *Orai1*$^{KI/KI}$ mice is less pronounced than the defect in T cells differentiated *in vitro* (Fig. 3E, Supplemental Fig. 3D) suggesting that the molecular composition of the CRAC channel may change during T cell differentiation.

Comparable SOCE defect in naive and memory T cells from *Orai1*$^{KI/KI}$ mice *in vivo*

To test this hypothesis and to compare the role of ORAI1 in naive and antigen-experienced memory T cells *in vivo*, we measured SOCE in CD62L^{+} CD44^{lo} naive and CD62L^{-} CD44^{hi} memory CD4^{+} T cells freshly isolated from *Orai1*$^{KI/KI}$ and wildtype control mice. Thapsigargin-induced SOCE, measured either as the peak of the Ca^{2+} response or the rate of Ca^{2+} influx, was significantly impaired in both naïve and memory T cells from *Orai1*$^{KI/KI}$ mice compared to wildtype controls (Fig. 4A–C, Supplemental Fig. 3). The peak and steady-state Ca^{2+} levels are important determinants of Ca^{2+} dependent cellular responses, while the Ca^{2+} influx rate provides an indirect read-out for CRAC channel function in the absence of direct electrophysiological measurements. Significantly reduced Ca^{2+} influx rates in T cells from *Orai1*$^{KI/KI}$ mice indicate that ORAI1 is a major store-operated Ca^{2+} entry channel in both naive and memory T cells *in vivo.* Other Ca^{2+} channels such as ORAI2 and ORAI3 are likely to contribute to SOCE as well given the residual Ca^{2+} influx in naive and memory T cells from *Orai1*$^{KI/KI}$ mice. We therefore compared mRNA expression levels of ORAI1, ORAI2 and ORAI3 using quantitative real-time PCR in CD62L^{+} CD44^{lo} naive and CD62L^{-} CD44^{hi} memory CD4^{+} and CD8^{+} T cells from wildtype C57BL/6 mice. ORAI1 and ORAI3 transcript levels were moderately higher in memory compared to naive CD4^{+} T cells (Fig. 4D). Importantly, the relative expression levels of all three ORAI paralogues were similar in naive and memory T cells. This is consistent with microarray gene expression data from C57BL/6 mice showing comparable expression of ORAI1, ORAI2 and ORAI3 (14, 28). ORAI2, ORAI3 or both are likely to contribute to SOCE in T cells given the residual Ca^{2+} influx in naive T cells from *Orai1*$^{KI/KI}$ mice and the concomitant mRNA expression of all three ORAI isoforms in naive T cells. Defining the precise contribution of ORAI2 and ORAI3 to Ca^{2+} influx in naive T cells from electrophysiological measurements alone is, however, difficult because the biophysical properties of all three ORAI isoforms are very similar (26). Collectively, our data show that ORAI1 is required for SOCE and CRAC channel function in T cells.

Strongly impaired T cell mediated skin allograft rejection in *Orai1*$^{KI/KI}$ mice

To investigate the role of ORAI1 for T cell function directly *in vivo*, we tested *Orai1*$^{KI/KI}$ mice in several models of T cell mediated immunity. We assessed the ability of *Orai1*$^{KI/KI}$ mice to reject skin allografts from MHC class I and class II mismatched mice which is generally considered to be mediated by both CD4^{+} and CD8^{+} T cells (29). Tail-skin grafts from BALB/c (H-2^{d}) mice were transplanted onto the back of *Orai1*$^{KI/KI}$ or *Orai1*$^{+/+}$ chimeric mice on the C57BL/6 background (H-2^{b}). Transplantation of tail skin to wildtype mice resulted in rejection of skin grafts with a median graft survival time of 13.7 days after skin transplantation (Fig. 5A). By contrast, *Orai1*$^{KI/KI}$ mice showed significantly prolonged skin allograft survival with a median graft survival of 21.1 days. Five days after transplantation, skin grafted onto wildtype C57BL/6 mice in general showed more pronounced perivascular leukocyte infiltration and occlusion of blood vessels – criteria for rejection of skin allografts (30) – compared to *Orai1*$^{KI/KI}$ recipient mice (Fig. 5B). Although both wildtype and *Orai1*$^{KI/KI}$ mice eventually rejected the allograft, the prolonged graft survival in *Orai1*$^{KI/KI}$ mice indicates that CD4^{+} and CD8^{+} T function *in vivo* are significantly impaired in the absence of functional ORAI1.

Delayed type hypersensitivity response is impaired in *Orai1*$^{KI/KI}$ mice

T_H2 cells mediate contact hypersensitivity reactions in response to exposure of epidermal skin cells to contact allergens (31). We tested whether *Orai1*$^{KI/KI}$ mice can mount a delayed type hypersensitivity response following sensitization with fluorescein isothiocyanate (FITC). Six days after *Orai1*$^{KI/KI}$ and control mice had been sensitized epicutaneously with FITC, their ears were painted with FITC or vehicle alone to elicit an immune response. Without prior sensitization, neither control nor *Orai1*$^{KI/KI}$ mice showed a contact

hypersensitivity response upon exposure to FITC. Sensitized wildtype mice showed a robust increase in ear thickness 24 hours after FITC treatment relative to the ear thickness before FITC treatment (Fig. 5C). By contrast, no ear swelling was detectable in FITC sensitized *Orai1*$^{KI/KI}$ mice in response to FITC. These findings indicate that T-cell mediated delayed type hypersensitivity responses and T_H2 cell function *in vivo* are significantly impaired in *Orai1*$^{KI/KI}$ mice.

Adoptively transferred CD4$^+$ T cells from *Orai1*$^{KI/KI}$ mice fail to induce colitis

Autoreactive T cells mediate inflammation and destruction of target tissues in numerous forms of autoimmune disease including colitis. Transfer of naive CD4$^+$ CD25$^-$ CD45RB$^+$ T cells into lymphopenic mice causes severe inflammatory bowel disease (IBD) in recipient animals. IBD develops in response to activation of naive T cells to stimulation by the gut microflora and their differentiation into proinflammatory T_H1 and T_H17 cells that goes unopposed due to the lack of Foxp3$^+$ regulatory T cells (T_{reg}) (32–34). We tested whether T cells from *Orai1*$^{KI/KI}$ mice are able to induce IBD. 5x10^5 CD4$^+$ CD25$^-$ CD45RB$^+$ T cells from *Orai1*$^{KI/KI}$ and wildtype *Orai1*$^{+/+}$ mice were transferred into syngeneic Rag2$^{-/-}$ mice. Mice that had received naive T cells from *Orai1*$^{+/+}$ mice progressively lost weight in contrast to recipients of *Orai1*$^{KI/KI}$ T cells which actually gained weight in the 12 weeks after adoptive T cell transfer (Fig. 6A). Whereas colons of wildtype recipients showed severe signs of inflammation on macroscopic and histological inspection, the colons of mice that had received *Orai1*$^{KI/KI}$ T cell were only moderately inflamed and showed few signs of epithelial hyperplasia, loss of goblet cells or ulceration (Fig. 6B–D). A similar resistance to autoimmune colitis was observed in recipient mice that had received CD4$^+$ CD25$^-$ CD45RB$^+$ T cells from *Stim1*$^{fl/fl}$ *Cd4Cre* mice that lack STIM1 expression and SOCE in T cells (Fig. 6E–F)(20) suggesting that STIM1 and ORAI1 are similarly important for the ability of T cells to induce inflammation *in vivo*. IFN-γ and IL-17 produced by CD4$^+$ T cells in the lamina propria of mice with IBD are critical mediators of inflammation (32). We therefore analyzed proinflammatory cytokine gene expression in cells isolated from mesenteric lymph nodes and colon explants of *Rag2*$^{-/-}$ recipients. Levels of IFN-γ, IL17A and TNF-α were strongly reduced in anti-CD3 stimulated cells isolated from mesenteric lymph nodes of mice that had received T cells from *Orai1*$^{KI/KI}$ mice compared to those that had received *Orai*$^{+/+}$ T cells (Fig. 6G). In addition, IFN-γ and IL17A mRNA expression levels in homogenates of resected colons from mice transferred with *Orai1*$^{KI/KI}$ T cells were barely detectable in contrast to mice that had received wildtype T cells (Fig. 6H). Taken together, the inability of T cells from *Orai1*$^{KI/KI}$ mice to cause autoimmune colitis is likely due to their failure to express proinflammatory cytokines. Defects in the expansion and/or homeostasis of ORAI1 deficient proinflammatory T cells may also contribute to the reduced levels of proinflammatory cytokines and protection from colitis as indicated by the reduced numbers of CD4$^+$ T cells in the mesenteric lymph nodes of mice that had received *Orai1*$^{KI/KI}$ T cells compared to those mice that had received wildtype T cells (Fig. 6I). The majority of *Orai1*$^{KI/KI}$ and wildtype T cells in lymph nodes showed a memory phenotype (CD44$^+$ CD62L$^-$) indicating that they had been activated *in vivo*. Collectively, these findings show that ORAI1 is critical for T cell activation *in vivo* and T cell mediated immune responses.

Impaired cytokine production in CD4$^+$ and CD8$^+$ T cells from *Orai1*$^{KI/KI}$ mice

To assess the role of ORAI1 for T cell function in more detail, we measured expression of cytokines in CD4$^+$ and CD8$^+$ T cells isolated from *Orai1*$^{KI/KI}$ mice that were grown *in vitro* under non-polarizing conditions (T_HN). T cells restimulated with PMA and ionomycin showed a severe defect in IL-2, IFN-γ and IL-4 production whereas expression of IL-10 was only partially impaired (Fig. 7A–B). The almost complete lack of IL-4 expression in ORAI1 deficient T cells is consistent with impaired T_H2 mediated contact hypersensitivity

responses in *Orai1*$^{KI/KI}$ mice. In addition to CD4$^+$ T cells, CD8$^+$ T cells from *Orai1*$^{KI/KI}$ mice that were differentiated into cytotoxic T cells *in vitro* also showed a severe defect in IFN-γ production upon restimulation (Fig. 7C). It is noteworthy, that the level of cytokine production in CD4$^+$ and CD8$^+$ T cells from *Orai1*$^{KI/KI}$ mice was comparable to that observed in *Orai1*$^{+/+}$ control T cells stimulated in the presence of cyclosporin A, an inhibitor of the Ca^{2+}/calmodulin dependent phosphatase calcineurin (Fig. 7B–C), suggesting that SOCE present in *Orai1*$^{KI/KI}$ T cells is below the threshold for Ca^{2+} dependent activation of calcineurin. The dramatic defect in cytokine production observed in ORAI1 deficient T cells differentiated *in vitro* is consistent with the almost complete lack of detectable IFN-γ and IL-17 production in *Orai1*$^{KI/KI}$ T cells isolated from Rag2$^{-/-}$ mice and the absence of colitis in these mice (Fig. 6).

In vitro proliferation of T cells from *Orai1*$^{KI/KI}$ mice is unperturbed

T cells from human patients homozygous for the ORAI1-R91W mutation showed a similar defect in cytokine gene expression as T cells from *Orai1*$^{KI/KI}$ mice and failed to proliferate *in vitro* (6,12,35). In the colitis experiments described above, we had observed reduced numbers of CD4$^+$ T cells in mesenteric lymph nodes of *Orai1*$^{KI/KI}$ T cell transferred mice, potentially due to a defect in T cell proliferation *in vivo* (Fig. 6I). To test this hypothesis, we isolated CD4$^+$ and CD8$^+$ T cells from lymph nodes of *Orai1*$^{KI/KI}$ and *Orai1*$^{+/+}$ control mice and restimulated them *in vitro* for 72h with αCD3 and αCD28. *Orai1*$^{KI/KI}$ T cells, however, proliferated as vigorously as T cells from littermate controls (Fig. 7D). Only when CD4$^+$ and CD8$^+$ T cells were first differentiated *in vitro* for 3 days and subsequently restimulated for 72h with αCD3 and αCD28 did *Orai1*$^{KI/KI}$ T cells fail to expand as vigorously as wildtype control T cells (Fig. 7E–F, left panels). Impaired proliferation of *in vitro* differentiated compared to naive *Orai1*$^{KI/KI}$ T cells is consistent with their more pronounced defect in SOCE (Fig. 3E). Treatment of wildtype and *Orai1*$^{KI/KI}$ CD4$^+$ and CD8$^+$ T cells with cyclosporin A completely blocked their proliferation (Fig. 7E–F, right panels). Taken together, these findings suggest that residual SOCE in T cells from *Orai1*$^{KI/KI}$ mice is sufficient to induce Ca^{2+}/calcineurin dependent cell proliferation but not cytokine gene expression.

Normal T and B cell development in *Orai1*$^{KI/KI}$ mice and partially impaired function of T_{reg} cells

As indicated further above, the numbers of T and B cells in spleen and lymph nodes of *Orai1*$^{KI/KI}$ chimeric mice were comparable to those in wildtype *Orai1*$^{+/+}$ mice (Fig. 1G, Supplemental Fig. 7A), suggesting that gross T and B cell development is unperturbed in ORAI1 deficient mice. When we analyzed populations of immature T cells in the thymus directly, we found comparable percentages of double negative (CD4$^-$CD8$^-$), double positive (CD4$^+$CD8$^+$) and single positive (CD4$^+$ or CD8$^+$) thymocytes in *Orai1*$^{KI/KI}$ and *Orai1*$^{+/+}$ wildtype mice (Fig. 8A). *Orai1*$^{KI/KI}$ thymocytes expressed similar levels of the TCRβ chain and the activation marker CD69 compared to control mice (Supplemental Fig. 6B). In addition, B cell maturation appeared normal in ORAI1 deficient mice as the numbers of mature AA4.1$^-$ and IgM$^-$ IgD$^+$ B cells in the spleens of *Orai1*$^{KI/KI}$ and *Orai1*$^{+/+}$ mice were similar (Supplemental Fig. 7B–E). Collectively these findings indicate that ORAI1 function is dispensable for lymphocyte development consistent with similar findings in mice lacking ORAI1 and STIM1 expression (16,20,36) and normal numbers of peripheral blood lymphocytes in ORAI1 and STIM1 deficient human patients (10,11,14).

In contrast to conventional T cells, the development of T_{reg} cells appears to be more dependent on SOCE. While *Orai1*$^{-/-}$ and *Stim1*$^{-/-}$ mice had normal development of conventional and regulatory T cells (16,17,36), mice with T cell specific deletion of both STIM1 and STIM2 have severely reduced numbers of T_{reg} but not conventional T cells (20)

suggesting that SOCE is required for T_{reg} development. *Orai1*$^{KI/KI}$ mice had numbers of $CD25^+$ $Foxp3^+$ T_{reg} cells in thymus, lymph nodes and spleen that were comparable to those in *Orai1*$^{+/+}$ controls consistent with the incomplete SOCE defect in naive *Orai1*$^{KI/KI}$ $CD4^+$ T cells (Fig. 8B). *Orai1*$^{KI/KI}$ T_{reg} cells did, however, show a reduced ability to suppress proliferation of conventional T cells *in vitro* compared to T_{reg} cells from *Orai1*$^{+/+}$ control mice (Fig. 8C). This defect in T_{reg} mediated suppression in *Orai1*$^{KI/KI}$ T cells is less pronounced than that observed in STIM1/STIM2 deficient T_{reg} cells (20) indicating that T_{reg} function is modulated by the strength of the Ca^{2+} signal provided by SOCE.

Discussion

We generated ORAI1-R93W homozygous knock-in mice to mimic an inherited human ORAI1 mutation that abolishes CRAC channel function and causes severe immunodeficiency in order to gain a detailed understanding of the role of ORAI1 for immune responses *in vivo* (10,12). In this study we show that ORAI1 is critically important for CRAC channel function and store-operated Ca^{2+} influx in T cells, that T cells from *Orai1*$^{KI/KI}$ mice have functional defects including impaired cytokine expression and T_{reg} mediated suppression and, most importantly, that ORAI1 is required for cell mediated immune responses *in vivo* such as T cell dependent allograft rejection, hypersensitivity responses and autoimmunity.

Lack of ORAI1 function in human T cells results in life-threatening immunodeficiency and recurrent infections due to impaired SOCE in T cells and potentially other immune cells (19). A role for ORAI1 in other T cell mediated immune responses *in vivo* has not been defined. We here show that *Orai1*$^{KI/KI}$ mice tolerate allogeneic skin grafts significantly longer than wildtype mice. Rejection of MHC class I and class II mismatched skin allografts is mediated by both $CD4^+$ and $CD8^+$ T cells (29) indicating that in *Orai1*$^{KI/KI}$ mice $CD4^+$ and $CD8^+$ T cell function is severely compromised. Since $CD4^+$ T cells alone are able to reject MHC class I and class II mismatched skin grafts in mice lacking $CD8^+$ T cells (37,38), attenuated allograft rejection in *Orai1*$^{KI/KI}$ mice furthermore suggests an important role for ORAI1 in $CD4^+$ T cell function *in vivo*. In addition, T_H2 mediated skin contact hypersensitivity responses were absent in *Orai1*$^{KI/KI}$ mice consistent with impaired IL-4 production in T cells from *Orai1*$^{KI/KI}$ mice *in vitro*.

Orai1$^{KI/KI}$ mice showed severely compromised proinflammatory T_H1 and T_H17 responses *in vivo*, apparent in the inability of T cells from ORAI1 deficient mice to induce colitis in an adoptive transfer model of inflammatory bowel disease. *Orai1*$^{KI/KI}$ T cells found in mesenteric lymph nodes and the colon failed to express IL-17A and IFN-γ that are required to induce colitis (32,39). In mice that had received wildtype $CD4^+$ $CD45RB^+$ T cells the IFN-γ secreted by T_H1 cells present in the inflamed colon results in activation of macrophages that in turn release proinflammatory IL-12 and TNF-α (39). A similar role for T_H17 cells and the RORγ dependent production of IL-17A and IL-17F was recently described in the pathogenesis of intestinal inflammation following transfer of $CD4^+$ $CD45RB^+$ naive T cells (32). Treatment of mice with anti-IFN-γ antibodies or IL-10 and neutralizing anti-IL17A antibodies, respectively, inhibited disease (32,39). The lack of IFN-γ and IL-17A expression in *Orai1*$^{KI/KI}$ T cells is very likely to be responsible for their failure to induce colitis in the adoptive transfer model we used to evaluate the role of ORAI1 for proinflammatory T cell function *in vivo*. In addition, numbers of transferred $CD4^+$ *Orai1*$^{KI/KI}$ T cells were reduced in the mesenteric lymph nodes of recipient mice. Impaired ORAI1 function does not interfere with proliferation of naive mouse T cells *in vitro* (Fig. 7), which is consistent with similar findings in *Orai1*$^{-/-}$ (16) and *Stim1*$^{-/-}$ (36) mice. We recently found, however, that STIM1 deficient T_H17 cells failed to expand *in vitro* and *in vivo* and are compromised in the expression of cytokines and cytokine receptors required for

T_H17 differentiation (40). A similar defect in the homeostasis of *Orai1*$^{KI/KI}$ T_H17 cells may contribute to their inability to induce colitis following adoptive transfer. Taken together, our findings demonstrate that ORAI1 mediated Ca^{2+} influx is required for the function of several T cell subsets *in vivo* in the context of T cell mediated hypersensitivity, autoimmunity and allograft rejection. These findings raise the possibility that many other aspects of T cell mediated immunity such as anti-viral and anti-tumor responses are also compromised in ORAI1 deficient mice, an issue that will have to be investigated in future studies.

The inability of T cells from *Orai1*$^{KI/KI}$ mice to mediate classical T cell dependent immune responses *in vivo* is explained to a large degree by their defective production of a number of key cytokines such as the proinflammatory IFN-γ, IL-17 and TNF-α and the T_H2 cytokine IL-4. The important role of ORAI1 for cytokine gene expression is emphasized by the almost complete absence of these cytokines upon restimulation of *Orai1*$^{KI/KI}$ T cells *in vitro* and the fact that stimulation of wildtype T cells in the presence of the calcineurin inhibitor CsA resulted in a comparable inhibition of cytokine expression. This finding suggests that SOCE in *Orai1*$^{KI/KI}$ T cells is not sufficient for the Ca^{2+} dependent activation of calcineurin which appears to depend entirely on Ca^{2+} influx through ORAI1. Other factors that contribute to the defect in T cell mediated immunity in *Orai1*$^{KI/KI}$ mice could be related to a role of ORAI1 in degranulation of mast cells (17), cytotoxic T cells and NK cells, as well as a potential role for SOCE in the differentiation and homeostasis of T_H17 cells (40).

Surprisingly however, T cells isolated from spleen and lymph nodes of *Orai1*$^{KI/KI}$ mice showed normal proliferative responses upon TCR stimulation. This is in contrast to impaired proliferation of T cells isolated from peripheral blood of ORAI1 deficient patients (8–10,35). The discrepancy could be due to differential Ca^{2+} signaling requirements in mouse and human T cells with regard to proliferation as T cells from STIM1 deficient mice proliferated normally *in vitro* (20,36) whereas those of STIM1 deficient patients did not (11). Proliferation of *Orai1*$^{KI/KI}$ T cells is unlikely to result from their residual SOCE and the potential contribution of other ORAI isoforms to SOCE in mouse T cells as STIM1 deficient murine T cells proliferated normally despite the absence of measurable Ca^{2+} influx in these cells (20,36). Nonetheless, while murine ORAI1 deficient T cells proliferated normally *in vitro*, we cannot currently exclude that T cell homeostasis *in vivo* is compromised in *Orai1*$^{KI/KI}$ mice given that numbers of *Orai1*$^{KI/KI}$ $CD4^+$ T cells were reduced in mesenteric lymph nodes of mice in which colitis had been induced by adoptive transfer of naive T cells.

In contrast to impaired T cell function, T and B cell development appeared normal in *Orai1*$^{KI/KI}$ mice which is consistent with normal lymphocyte development in *Orai1*$^{-/-}$ (16,17), and *Stim1*$^{-/-}$ mice (20,36) as well as human ORAI1 (8–10,35) and STIM1 (11) deficient patients which present with normal lymphocyte numbers and subsets in their peripheral blood. It should be pointed out that normal T cell development in *Orai1*$^{KI/KI}$ mice as described here refers to numbers of T cells and T cell subsets only as we have not analyzed TCR repertoire selection in these mice. We cannot currently exclude that thymic selection of *Orai1*$^{KI/KI}$ T cells is altered due to impaired Ca^{2+} signaling. Several indirect lines of evidence suggest that Ca^{2+} signals are required for proper T cell development in the thymus including Ca^{2+} oscillations observed in T cells undergoing positive selection (41), defects in positive selection of thymocytes in mice lacking the calcineurin B1 regulatory subunit (42) and the fact that ORAI1 is expressed at all stages during thymocyte development (14). Given the normal T cell development in ORAI1 (16,17) and STIM1 (11,20,36) deficient mice and human patients it appears, however, that the STIM1/ORAI1 pathway is dispensable for lymphocyte development, and raises the possibility that other Ca^{2+} entry channels mediate this process (for a more detailed discussion refer to (43)).

The importance of ORAI1 for CRAC channel function in lymphocytes is evident from the clinical immunodeficiency and severely impaired SOCE in T and B cells from patients with mutations in ORAI1 that result in either non-functional channel protein (12) or abolished ORAI1 expression (10). Deletion of *Orai1* in mice has led to conflicting results as to the role of ORAI1 for SOCE in mouse T cells. One study showed impaired SOCE and CRAC channel currents in T cells from *Orai1*$^{-/-}$ mice resulting in impaired cytokine gene expression (16), whereas another study found that deletion of *Orai1* did not affect SOCE in T cells and only moderately impaired cytokine production (17). Analyzing naive and differentiated T cells from *Orai1*$^{KI/KI}$ mice we found that ORAI1 is required for SOCE and CRAC channel function in mouse T cells as naive CD4^{+} and CD8^{+} T cells from *Orai1*$^{KI/KI}$ fetal liver chimeras showed impaired SOCE compared to wildtype controls. An even more pronounced defect with very low residual SOCE and CRAC channel currents was observed in CD4^{+} and CD8^{+} T cells differentiated *in vitro*. This finding suggested that the configuration of the CRAC channel complex may change during T cell differentiation from naïve to antigen experienced effector T cells with ORAI1 being the predominant ORAI isoform in effector T cells. We did observe, however, a comparable SOCE defect in naïve (CD62L^{+}CD44^{lo}) and memory (CD62L^{-}CD44^{hi}) CD4^{+} T cells isolated from *Orai1*$^{KI/KI}$ mice. It remains to be determined whether the composition of CRAC channel alters between distinct lymphocyte subsets.

The residual SOCE and Ca^{2+} current in T cells from *Orai1*$^{KI/KI}$ mice we observed were not due to vestigial function of the mutant ORAI1-R93W protein because residual I_{CRAC} in *Orai1*$^{KI/KI}$ T cells was comparable to that observed in T cells from *Orai1*$^{-/-}$ mice (16) and because T cells from patients homozygous for the equivalent ORAI1-R91W mutation lack I_{CRAC} completely (12,13). Thus residual SOCE in naïve *Orai1*$^{KI/KI}$ T cells is likely to be due to – as has been suggested – ORAI2 or ORAI3 function, consistent with the observed expression of ORAI2 and ORAI3 mRNA expression in naïve CD4^{+} T cells (16,17). ORAI2 has been proposed to be the dominant ORAI isoform in naive T cells as ORAI2 mRNA levels in these cells were reported to vastly exceed those of ORAI1 or ORAI3 (17). By contrast, our quantitative mRNA expression analysis indicates that all three ORAI isoforms are expressed at roughly comparable levels. This is consistent with Northern blot (16,17) and microarray (14,28) data from naive T cells showing comparable ORAI1 and ORAI2 mRNA levels that were moderately higher than those for ORAI3.

It proved to be difficult to evaluate by electrophysiological means whether residual SOCE and Ca^{2+} currents in *Orai1*$^{KI/KI}$ T cells are due to ORAI2 or ORAI3 function, because the biophysical properties of all three ORAI isoforms are very similar under overexpression conditions (26,27) and are insufficiently defined for endogenous ORAI channels. The biophysical properties of residual Ca^{2+} currents in T cells from *Orai1*$^{KI/KI}$ mice were indistinguishable from native CRAC channel currents and those in cells ectopically expressing ORAI1. Currents did not show any of the properties observed in cells ectopically expressing ORAI2 such as lack of slow inactivation of Ca^{2+} currents (26,27) or ORAI3 such as potentiation of Ca^{2+} currents with 50 μM 2-APB (26). Although 2-APB potentiation of native ORAI3 currents was recently described in breast cancer cells (44), the properties of overexpressed ORAI2 and ORAI3 channels may not accurately mimic those of endogenous ORAI2 and ORAI3 CRAC currents in T cells. In summary, I_{CRAC} in naive and differentiated murine T cells is in large part due to ORAI1. Although ORAI2 and ORAI3 are expressed in these cells, their contribution to CRAC channel function and T cell mediated immune responses remains to be determined.

A surprising difference between human patients and mice homozygous for the equivalent ORAI1-R91W and -R93W mutations, respectively, is the neonatal lethality observed in *Orai1*$^{KI/KI}$ mice but not human patients (10). ORAI1 deficient patients generally succumb to

immunodeficiency in their first year of life but do survive following treatment by hematopoietic stem cell transplantation. Neonatal lethality in *Stim1*$^{-/-}$ mice has been attributed to a myopathy characterized by morphological and functional abnormalities in skeletal myotubes (25). This finding is intriguing because human ORAI1 and STIM1 deficient patients suffer from congenital muscular hypotonia that in a patient with ORAI1-R91W mutation was associated with the histological observation of atrophic type II muscle fibers (10,11). Newborn *Orai1*$^{KI/KI}$ pups, however, lacked obvious signs of gross muscular dysfunction apart from their inability to feed and death due to dehydration within ~ 12h post partum. Structurally, their skeletal muscles appeared normal although a small fraction (< 5%) of muscle fibers contained 'swollen' mitochondria in transmission electron microscopy reminiscent of the mitochondriopathy observed in *Stim1* deficient mice (25). It is unlikely, however, that the ultrastructural abnormalities observed in a small minority of muscle cells account for the neonatal lethality of *Orai1*$^{KI/KI}$ mice, which is consistent with the observation that transgenic mice with skeletal muscle specific expression of a dominant negative mutant of ORAI1 are viable (45).

It is noteworthy that the phenotype of *Orai1*$^{KI/KI}$ mice is more severe than that observed in *Orai1*$^{-/-}$ mice in several respects raising the possibility that the mutant ORAI1-R93W protein exerts an inhibitory effect on other Ca^{2+} channels such as ORAI2 and ORAI3. The mutant ORAI1-R91W protein is expressed in cells and can interact with wildtype ORAI1 (assessed by coimmunoprecipitation and fluorescence resonance energy transfer (FRET) experiments; Supplemental Fig. 5) in what is likely to be a tetrameric CRAC channel complex composed of four ORAI1 subunits (4). Alternatively, ORAI1 might form a tetrameric complex with other ORAI proteins as it was shown to be able to physically interact with ORAI2 and ORAI3 (26, 46) and to form heteromeric Ca^{2+} channels when co-expressed with ORAI3 (47). The following observations suggest that the mutant ORAI1-R93W protein may exert an additional inhibitory effect on SOCE compared to cells "simply" lacking ORAI1 expression. (i) *Orai1*$^{KI/KI}$ mice on a mixed genetic background (ICR) show a more severe, essentially non-rescuable neonatal lethality (Fig. 1) compared to *Orai1*$^{-/-}$ (ICR) mice (16) and *Orai1*$^{-/-}$ mice that were generated on a mixed genetic background (15, 17). (ii) Cytokine production, especially that of IL-2, is more severely impaired in $CD4^+$ T cells from *Orai1*$^{KI/KI}$ than *Orai1*$^{-/-}$ mice (Fig. 7) (16, 17). (iii) Residual SOCE in naïve $CD4^+$ and $CD8^+$ T cells from *Orai1*$^{KI/KI}$ mice is lower than that in *Orai1*$^{-/-}$ T cells (Fig. 3) (16). By contrast, *in vitro* differentiated T_HN cells from *Orai1*$^{KI/KI}$ and *Orai1*$^{-/-}$ mice had comparable residual I_{CRAC} amplitudes as expected for cells in which ORAI1 is the predominant ORAI1 isoform (16). (iv) *Orai1*$^{KI/+}$ T cells heterozygous for the R93W mutation show CRAC currents (in 20 mM extracellular Ca^{2+}) that are ~ 30% of those in wildtype T cells (Supplemental Fig. 4B–D), slightly less than expected for a "simple" loss-of-function mutant. A dominant negative effect of mutant ORAI1-R91W on CRAC channel function was postulated by Thompson et al. who showed that incorporating one mutant ORAI1-R91W subunit together with three wildtype subunits in a concatenated tetramer reduced I_{CRAC} by ~ 50%; two mutant subunits decreased I_{CRAC} by > 90% (48). We speculate that nonfunctional ORAI1-R93W (or R91W in human) might be incorporated into heteromeric CRAC channel complexes containing ORAI2 and ORAI3 (although these have not been demonstrated to exist except under overexpression conditions), thereby preventing ORAI2 or ORAI3 from rescuing SOCE.

We here show that ORAI1 is essential for SOCE and CRAC channel currents in T cells and that in the absence of ORAI1 function in *Orai1*$^{KI/KI}$ mice, T cell mediated immunity is severely impaired both *in vitro* and *in vivo*. Interfering with Ca^{2+} influx through inhibition of ORAI1 function may therefore be useful to suppress unwanted immune responses in the context of transplant rejection, inflammation and autoimmunity.

Supplementary Material

Refer to Web version on PubMed Central for supplementary material.

Acknowledgments

We thank Dr. Klaus Rajewsky and his lab for help with the generation of Orai1 knock-in mice. We thank Dr. Fengxia Liang and Tim Macatee for technical assistance with transmission electron microscopy and histological analysis, respectively.

Abbreviations used in this paper

CRAC	calcium release activated calcium
FLC	fetal liver chimeras
SOCE	store-operated calcium entry
STIM1	stromal interaction molecule 1

References

1. Feske S. Calcium signalling in lymphocyte activation and disease. Nat Rev Immunol. 2007; 7:690–702. [PubMed: 17703229]
2. Lewis RS. The molecular choreography of a store-operated calcium channel. Nature. 2007; 446:284–287. [PubMed: 17361175]
3. Prakriya M. The molecular physiology of CRAC channels. Immunol Rev. 2009; 231:88–98. [PubMed: 19754891]
4. Hogan PG, Lewis RS, Rao A. Molecular basis of calcium signaling in lymphocytes: STIM and ORAI. Annu Rev Immunol. 2010; 28:491–533. [PubMed: 20307213]
5. Cahalan MD. STIMulating store-operated Ca(2+) entry. Nat Cell Biol. 2009; 11:669–677. [PubMed: 19488056]
6. Feske S, Giltnane J, Dolmetsch R, Staudt LM, Rao A. Gene regulation mediated by calcium signals in T lymphocytes. Nat Immunol. 2001; 2:316–324. [PubMed: 11276202]
7. Oh-hora M, Rao A. Calcium signaling in lymphocytes. Curr Opin Immunol. 2008; 20:250–258. [PubMed: 18515054]
8. Le Deist F, Hivroz C, Partiseti M, Thomas C, Buc HA, Oleastro M, Belohradsky B, Choquet D, Fischer A. A primary T-cell immunodeficiency associated with defective transmembrane calcium influx. Blood. 1995; 85:1053–1062. [PubMed: 7531512]
9. Partiseti M, Le Deist F, Hivroz C, Fischer A, Korn H, Choquet D. The calcium current activated by T cell receptor and store depletion in human lymphocytes is absent in a primary immunodeficiency. J Biol Chem. 1994; 269:32327–32335. [PubMed: 7798233]
10. McCarl CA, Picard C, Khalil S, Kawasaki T, Rother J, Papolos A, Kutok J, Hivroz C, Ledeist F, Plogmann K, Ehl S, Notheis G, Albert MH, Belohradsky BH, Kirschner J, Rao A, Fischer A, Feske S. ORAI1 deficiency and lack of store-operated Ca2+ entry cause immunodeficiency, myopathy, and ectodermal dysplasia. J Allergy Clin Immunol. 2009; 124:1311–1318. e1317. [PubMed: 20004786]
11. Picard C, McCarl CA, Papolos A, Khalil S, Luthy K, Hivroz C, LeDeist F, Rieux-Laucat F, Rechavi G, Rao A, Fischer A, Feske S. STIM1 mutation associated with a syndrome of immunodeficiency and autoimmunity. N Engl J Med. 2009; 360:1971–1980. [PubMed: 19420366]
12. Feske S, Gwack Y, Prakriya M, Srikanth S, Puppel SH, Tanasa B, Hogan PG, Lewis RS, Daly M, Rao A. A mutation in Orai1 causes immune deficiency by abrogating CRAC channel function. Nature. 2006; 441:179–185. [PubMed: 16582901]
13. Feske S, Prakriya M, Rao A, Lewis RS. A severe defect in CRAC Ca2+ channel activation and altered K+ channel gating in T cells from immunodeficient patients. J Exp Med. 2005; 202:651–662. [PubMed: 16147976]

14. Feske S. ORAI1 and STIM1 deficiency in human and mice: roles of store-operated Ca2+ entry in the immune system and beyond. Immunol Rev. 2009; 231:189–209. [PubMed: 19754898]
15. Braun A, Varga-Szabo D, Kleinschnitz C, Pleines I, Bender M, Austinat M, Bosl M, Stoll G, Nieswandt B. Orai1 (CRACM1) is the platelet SOC channel and essential for pathological thrombus formation. Blood. 2009; 113:2056–2063. [PubMed: 18832659]
16. Gwack Y, Srikanth S, Oh-Hora M, Hogan PG, Lamperti ED, Yamashita M, Gelinas C, Neems DS, Sasaki Y, Feske S, Prakriya M, Rajewsky K, Rao A. Hair loss and defective T- and B-cell function in mice lacking ORAI1. Mol Cell Biol. 2008; 28:5209–5222. [PubMed: 18591248]
17. Vig M, DeHaven WI, Bird GS, Billingsley JM, Wang H, Rao PE, Hutchings AB, Jouvin MH, Putney JW, Kinet JP. Defective mast cell effector functions in mice lacking the CRACM1 pore subunit of store-operated calcium release-activated calcium channels. Nat Immunol. 2008; 9:89–96. [PubMed: 18059270]
18. Bergmeier W, Oh-Hora M, McCarl CA, Roden RC, Bray PF, Feske S. R93W mutation in Orai1 causes impaired calcium influx in platelets. Blood. 2009; 113:675–678. [PubMed: 18952890]
19. Feske S, Picard C, Fischer A. Immunodeficiency due to mutations in ORAI1 and STIM1. Clin Immunol. 2010; 135:169–182. [PubMed: 20189884]
20. Oh-Hora M, Yamashita M, Hogan PG, Sharma S, Lamperti E, Chung W, Prakriya M, Feske S, Rao A. Dual functions for the endoplasmic reticulum calcium sensors STIM1 and STIM2 in T cell activation and tolerance. Nat Immunol. 2008; 9:432–443. [PubMed: 18327260]
21. Gaspari AA, Katz SI. Contact hypersensitivity. Curr Protoc Immunol. 2001; Chapter 4(Unit 4 2)
22. Moolenbeek C, Ruitenberg EJ. The “Swiss roll”: a simple technique for histological studies of the rodent intestine. Lab Anim. 1981; 15:57–59. [PubMed: 7022018]
23. Di L, Srivastava S, Zhdanova O, Ding Y, Li Z, Wulff H, Lafaille M, Skolnik EY. Inhibition of the K+ channel KCa3.1 ameliorates T cell-mediated colitis. Proc Natl Acad Sci U S A. 2010; 107:1541–1546. [PubMed: 20080610]
24. Navarro-Borelly L, Somasundaram A, Yamashita M, Ren D, Miller RJ, Prakriya M. STIM1-Orai1 interactions and Orai1 conformational changes revealed by live-cell FRET microscopy. J Physiol. 2008; 586:5383–5401. [PubMed: 18832420]
25. Stiber J, Hawkins A, Zhang ZS, Wang S, Burch J, Graham V, Ward CC, Seth M, Finch E, Malouf N, Williams RS, Eu JP, Rosenberg P. STIM1 signalling controls store-operated calcium entry required for development and contractile function in skeletal muscle. Nat Cell Biol. 2008; 10:688–697. [PubMed: 18488020]
26. Lis A, Peinelt C, Beck A, Parvez S, Monteilh-Zoller M, Fleig A, Penner R. CRACM1, CRACM2, and CRACM3 are store-operated Ca2+ channels with distinct functional properties. Curr Biol. 2007; 17:794–800. [PubMed: 17442569]
27. DeHaven WI, Smyth JT, Boyles RR, Putney JW Jr. Calcium inhibition and calcium potentiation of Orai1, Orai2, and Orai3 calcium release-activated calcium channels. J Biol Chem. 2007; 282:17548–17556. [PubMed: 17452328]
28. BioGPS. 2009. http://biogps.gnf.org
29. Youssef AR, Otley C, Mathieson PW, Smith RM. Role of CD4+ and CD8+ T cells in murine skin and heart allograft rejection across different antigenic desparities. Transpl Immunol. 2004; 13:297–304. [PubMed: 15589743]
30. Wolman M, Bleiberg I, Leibovici J. Histological criteria for immunological rejection of mouse skin homografts. J Pathol. 1977; 122:1–7. [PubMed: 328839]
31. Dearman RJ, Kimber I. Role of CD4(+) T helper 2-type cells in cutaneous inflammatory responses induced by fluorescein isothiocyanate. Immunology. 2000; 101:442–451. [PubMed: 11122447]
32. Leppkes M, Becker C, Ivanov, Hirth S, Wirtz S, Neufert C, Pouly S, Murphy AJ, Valenzuela DM, Yancopoulos GD, Becher B, Littman DR, Neurath MF. RORgamma-expressing Th17 cells induce murine chronic intestinal inflammation via redundant effects of IL-17A and IL-17F. Gastroenterology. 2009; 136:257–267. [PubMed: 18992745]
33. Izcue A, Coombes JL, Powrie F. Regulatory T cells suppress systemic and mucosal immune activation to control intestinal inflammation. Immunol Rev. 2006; 212:256–271. [PubMed: 16903919]

34. Ostanin DV, Bao J, Koboziev I, Gray L, Robinson-Jackson SA, Kosloski-Davidson M, Price VH, Grisham MB. T cell transfer model of chronic colitis: concepts, considerations, and tricks of the trade. Am J Physiol Gastrointest Liver Physiol. 2009; 296:G135–146. [PubMed: 19033538]
35. Feske S, Muller JM, Graf D, Kroczek RA, Drager R, Niemeyer C, Baeuerle PA, Peter HH, Schlesier M. Severe combined immunodeficiency due to defective binding of the nuclear factor of activated T cells in T lymphocytes of two male siblings. Eur J Immunol. 1996; 26:2119–2126. [PubMed: 8814256]
36. Beyersdorf N, Braun A, Vogtle T, Varga-Szabo D, Galdos RR, Kissler S, Kerkau T, Nieswandt B. STIM1-independent T cell development and effector function in vivo. J Immunol. 2009; 182:3390–3397. [PubMed: 19265116]
37. Zijlstra M, Auchincloss H Jr, Loring JM, Chase CM, Russell PS, Jaenisch R. Skin graft rejection by beta 2-microglobulin-deficient mice. J Exp Med. 1992; 175:885–893. [PubMed: 1552287]
38. Dalloul AH, Chmouzis E, Ngo K, Fung-Leung WP. Adoptively transferred CD4+ lymphocytes from CD8 −/− mice are sufficient to mediate the rejection of MHC class II or class I disparate skin grafts. J Immunol. 1996; 156:4114–4119. [PubMed: 8666777]
39. Powrie F, Leach MW, Mauze S, Menon S, Caddle LB, Coffman RL. Inhibition of Th1 responses prevents inflammatory bowel disease in scid mice reconstituted with CD45RBhi CD4+ T cells. Immunity. 1994; 1:553–562. [PubMed: 7600284]
40. Ma J, McCarl CA, Khalil S, Luethy K, Feske S. T-cell specific deletion of STIM1 and STIM2 protects mice from EAE by impairing the effector functions of TH1 and TH17 cells. Eur J Immun. 2010 in press.
41. Bhakta NR, Oh DY, Lewis RS. Calcium oscillations regulate thymocyte motility during positive selection in the three-dimensional thymic environment. Nat Immunol. 2005; 6:143–151. [PubMed: 15654342]
42. Neilson JR, Winslow MM, Hur EM, Crabtree GR. Calcineurin B1 is essential for positive but not negative selection during thymocyte development. Immunity. 2004; 20:255–266. [PubMed: 15030770]
43. Oh-hora M. Calcium signaling in the development and function of T-lineage cells. Immunol Rev. 2009; 231:210–224. [PubMed: 19754899]
44. Motiani RK, Abdullaev IF, Trebak M. A novel native store-operated calcium channel encoded by Orai3:Selective requirement of Orai3 versus Orai1 in estrogen receptor positive versus estrogen receptor negative breast cancer cells. J Biol Chem.
45. Lyfenko, AD.; Dirksen, RT. Molecular mechanisms of store-operated Ca2+ entry in adult mammalian skeletal muscle. Biophysical Society meeting; San Francisco. 2010. Platform M: Excitation-Contraction Coupling (1048-Plat)
46. Gwack Y, Srikanth S, Feske S, Cruz-Guilloty F, Oh-hora M, Neems DS, Hogan PG, Rao A. Biochemical and functional characterization of Orai proteins. J Biol Chem. 2007; 282:16232–16243. [PubMed: 17293345]
47. Schindl R, Frischauf I, Bergsmann J, Muik M, Derler I, Lackner B, Groschner K, Romanin C. Plasticity in Ca2+ selectivity of Orai1/Orai3 heteromeric channel. Proc Natl Acad Sci U S A. 2009; 106:19623–19628. [PubMed: 19887627]
48. Thompson JL, Mignen O, Shuttleworth TJ. The Orai1 severe combined immune deficiency mutation and calcium release-activated Ca2+ channel function in the heterozygous condition. J Biol Chem. 2009; 284:6620–6626. [PubMed: 19075015]

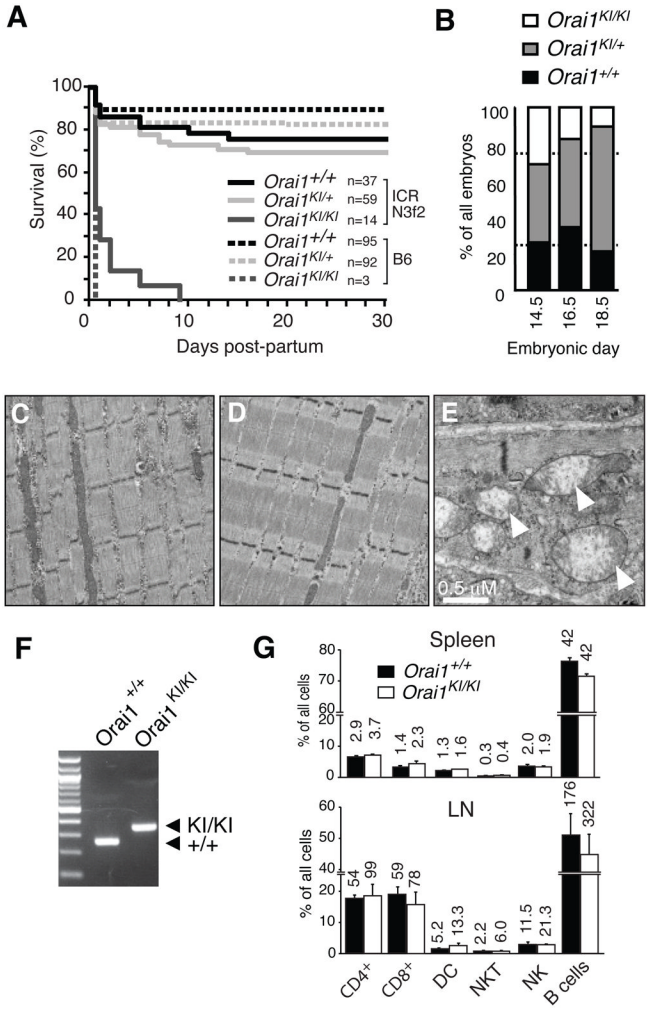

Fig. 1. Phenotype of homozygous *Orai1*$^{KI/KI}$ (knock-in) mice

A, Homozygous *Orai1*$^{KI/KI}$ mice are neonatally lethal on the C57BL/6 background. Mice heterozygous for the Orai1 mutation (*Orai1*$^{KI/+}$ on C57BL/6) were intercrossed or first crossed to the outbred ICR strain for 3 generations and then intercrossed. Homozygous *Orai1*$^{KI/KI}$ mice on the C57BL/6 background all died within ~ 12h post partum. A minority of outbred *Orai1*$^{KI/KI}$ (ICR N3f2) mice survived for up to 9 days post partum but was severely runted. Numbers (n) of mice per genotype analyzed are indicated. **B**, Moderately impaired embryonic development of *Orai1*$^{KI/KI}$ mice. Progeny of intercrossed *Orai1*$^{KI/+}$ (C57BL/6) mice were analyzed for genotype, viability and morphological abnormalities at E14.5 (n=42), E16.5 (n=29) and E18.5 (n=47) of gestation. The number of *Orai1*$^{KI/KI}$ embryos at E18.5 was reduced compared to a normal Mendelian distribution (indicated by dotted lines). **C–E**, Intact myofibril structure in *Orai1*$^{KI/KI}$ mice. Muscle fibers from the lower extremity of 7-day-old wildtype *Orai1*$^{+/+}$ (C) and *Orai1*$^{KI/KI}$ (D) mice (both ICR N3f2) were analyzed by transmission electron microscopy (magnification 11,500x). **E,** A minority of muscle fibers in the leg of 7-day-old *Orai1*$^{KI/KI}$ (ICR N3f2) mice contains enlarged mitchondria with dissolved cristae structure (arrow in E, magnification 19,500x). **F**, Fetal liver chimeric (FLC) mice were generated by transfer of fetal liver cells from *Orai1*$^{KI/KI}$ and *Orai1*$^{+/+}$ (C57BL/6) E14.5 mouse embryos to sublethally irradiated *Rag2*$^{-/-}$, *cγ* $^{-/-}$ mice. PCR based genotyping of CD4^{+} T cells from FLC mice identifies ~280 and ~320 bp bands for the wildtype *Orai1*$^{+/+}$ and targeted *Orai1*$^{KI/KI}$ locus containing

a loxP site, respectively (see Supplemental Fig. 1). **G,** *Orai1*$^{KI/KI}$ FLC mice have normal lymphocyte numbers in spleen and peripheral lymph nodes (LN). Numbers above bars indicate absolute numbers of cells in spleen (x10^6) and one peripheral LN (x10^3, averaged from 1–4 LNs harvested per mouse). Averages (± SEM) are from 4 mice per group.

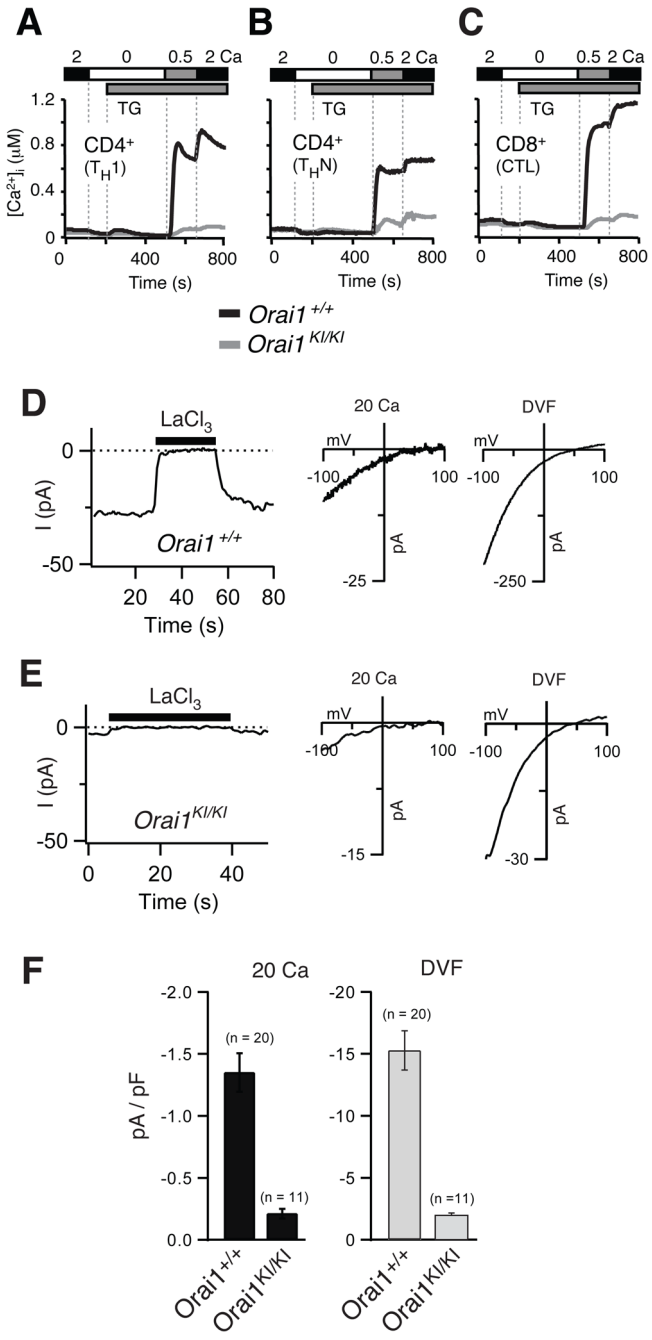

Fig. 2. Severe defect in SOCE and CRAC channel function in T cells from *Orai1*$^{KI/KI}$ mice

A–C, Severely impaired SOCE in T cells from *Orai1*$^{KI/KI}$ mice. CD4$^+$ T cells were differentiated *in vitro* into T_H1 cells (A) or non-polarized T_HN cells (B); CD8$^+$ T cells were differentiated into cytotoxic T cells (CTL, panel C). T cells were loaded with Fura-2 AM and stimulated with thapsigargin (TG) for measurements of $[Ca^{2+}]_i$. Traces show averages of 80–100 cells from one of 3–11 experiments in total. For a quantification see Supplemental Fig. 3A–C. **D–F**, Strongly reduced I_{CRAC} in T cells from *Orai1*$^{KI/KI}$ mice. Ca^{2+} and Na^+ CRAC currents were measured in CD4$^+$ T_HN cells from *Orai1*$^{KI/KI}$ and littermate control mice that were pretreated with 1 μM thapsigargin (TG) immediately before the recording to activate CRAC channels. **D–E**, Leak-corrected CRAC currents

measured during hyperpolarizing pulses to −100 mV plotted against time (left panels). The extracellular solution contained 20 mM Ca^{2+} in the absence or presence (black bar) of $LaCl_3$. *Right panels* show representative I–V plots of CRAC channel currents in 20 mM Ca^{2+} Ringer and Na^+-based divalent-free (DVF) solution, obtained from 100-ms voltage ramps from −100 to +100 mV. I–V plots show inward rectification and reversal potentials that are characteristic of well-defined native and ORAI1-encoded CRAC currents (3). **F**, Averages (±SEM) of peak current densities recorded in *Orai1*$^{KI/KI}$ and *Orai1*$^{+/+}$ control T_HN cells in 20 mM Ca^{2+} Ringer and DVF solution.

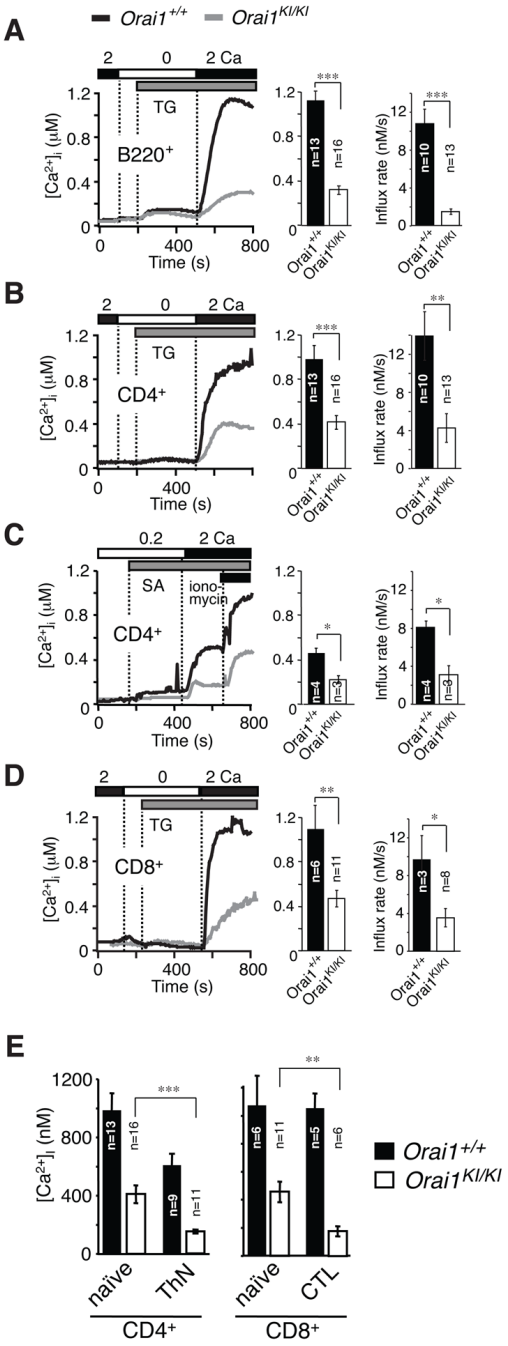

Fig. 3. Impaired SOCE in naïve T and B cells from *Orai1*$^{KI/KI}$ mice

A–D, Intracellular Ca^{2+} concentrations $[Ca^{2+}]_i$ were measured by time-lapse imaging in B cells (A) and T cells (B–D) isolated from lymph nodes of 5–6 week old *Orai1*$^{KI/KI}$ and wildtype *Orai1*$^{+/+}$ fetal liver chimeric mice. Cells were stimulated with thapsigargin (grey bars in A, B, D) or TCR crosslinking with anti-CD3-biotin and streptavidin (grey bar in C) in the presence of the indicated extracellular Ca^{2+} concentrations (in mM). Traces show averages of 80–100 cells from one representative experiment. Bar graphs show averages (±SEM) of peak Ca^{2+} concentrations and initial rates of Ca^{2+} influx (in the first 15s after Ca^{2+} readdition) from the indicated number of repeat experiments. TG, thapsigargin; SA, streptavidin. **E**, SOCE is more severely impaired in differentiated than naïve T cells from

Orai1$^{KI/KI}$ mice. Comparison of peak $[Ca^{2+}]_i$ in naïve versus *in vitro* differentiated $CD4^+$ (T_HN) and $CD8^+$ T cells (CTL) following TG stimulation and readdition of 2 mM extracellular Ca^{2+}. Bar graphs show averages (±SEM) from the indicated number of experiments. *, $p<0.05$; **, $p<0.005$; ***, $p<0.001$ (Student's t-test).

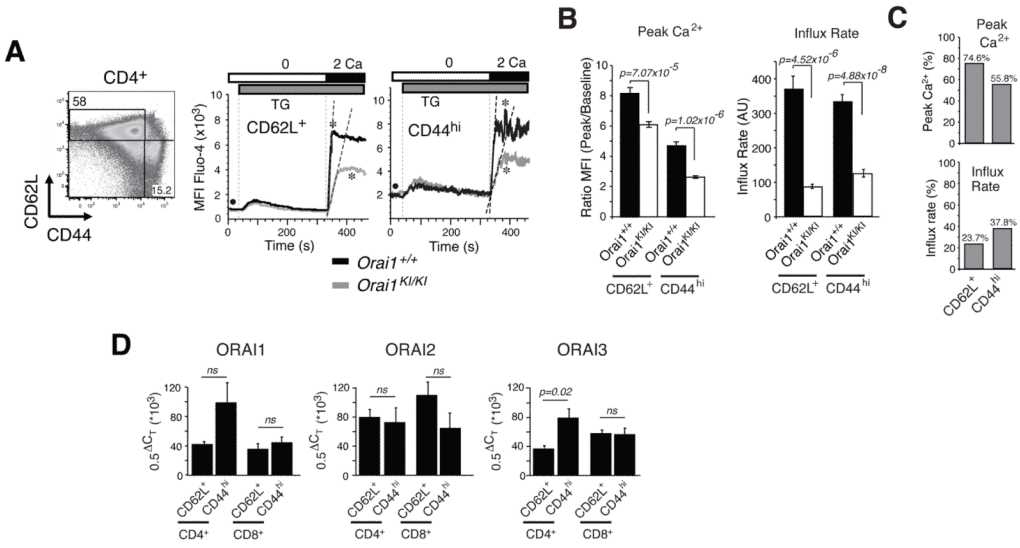

Fig. 4. SOCE defect in naive and memory CD4$^+$ T cells from *Orai1*$^{KI/KI}$ mice

A, For measurements of SOCE by flow cytometry, mononuclear cells were isolated from lymph nodes of *Orai1*$^{KI/KI}$ and *Orai1*$^{+/+}$ control mice, stained with antibodies to CD4, CD44 and CD62L, loaded with Fluo-4 and stimulated with thapsigargin (TG). Representative Ca^{2+} traces from naive CD4$^+$ CD62L$^+$ CD44^{lo} T cells (abbreviated as CD62L$^+$) and memory CD4$^+$ CD62L$^-$ CD44^{hi} T cells (abbreviated as CD44^{hi}). * indicates the peak Ca^{2+} response; • indicates baseline $[Ca^{2+}]_i$; dashed lines indicate initial rates of Ca^{2+} influx. **B,** Bar graphs show averages (±SEM) of peak Ca^{2+} responses (indicated by * in panel A) normalized to baseline (indicated by • in panel A) and initial rates of Ca^{2+} influx after readdition of 2 mM extracellular Ca^{2+} from n=13 (*Orai1*$^{+/+}$) and n=19 (*Orai1*$^{KI/KI}$) repeat experiments. p-values, Student's t-test. **C**, Peak Ca^{2+} levels and influx rates in *Orai1*$^{KI/KI}$ T cells in percent of values observed in wildtype T cells; derived from data in B. **D,** Comparable expression levels of ORAI1, ORAI2 and ORAI3 in naive and memory T cells. CD4$^+$ and CD8$^+$ naive CD62L$^+$ CD44^{lo} and memory CD62L$^-$ CD44^{hi} T cells from wildtype mice were sorted by FACS and analyzed by quantitative real-time PCR for mRNA expression of ORAI1, ORAI2 and ORAI3. Averages (±SEM) are from six repeat experiments (except for ORAI1 in CD8$^+$ CD62L$^-$CD44^{hi} T cells, n=3) performed in triplicates. ΔC_T, threshhold cycle differential. p-values, Student's t-test.

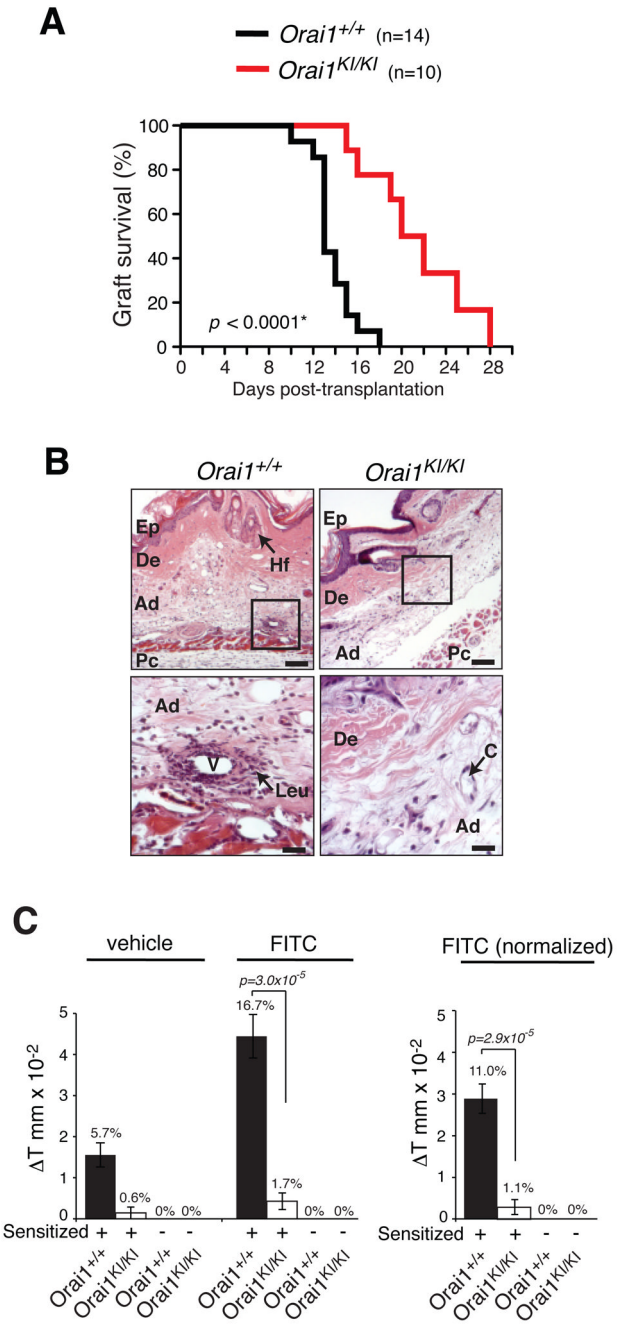

Fig. 5. Impaired T-cell mediated immunity in *Orai1*$^{KI/KI}$ mice *in vivo*

A, Mitigated skin allograft rejection in *Orai1*$^{KI/KI}$ mice. Tail-skin grafts from BALB/c mice (H-2^{d}) were transplanted onto the backs of *Orai1*$^{KI/KI}$ or *Orai1*$^{+/+}$ control FLC mice (C57BL/6, H-2^{b}). The size and integrity of the skin graft were scored daily and considered rejected when the grafted skin was < 20% of its original size. Plotted are the percentages of wildtype (n=14) and *Orai1*$^{KI/KI}$ (n=10) mice with intact allografts in days after transplantation. * p-value, logrank test. **B**, Histology of skin allografts in *Orai1*$^{KI/KI}$ and *Orai1*$^{+/+}$ mice five days after transplantation. Infiltration of leukocytes (Leu) around blood vessels (V) in the adipose layer (Ad) in *Orai1*$^{+/+}$ mice is indicated. Abbreviations: C, capillary; De, dermis; Ep, epidermis; Hf, hair follicle; Pc, panniculus carnosus.

Magnification and scale bars: 10x, 200 μm (top panels), 40x, 50 μm (bottom panels). **C,** Skin contact hypersensitivity response is impaired in *Orai1*$^{KI/KI}$ mice. *Orai1*$^{KI/KI}$ and *Orai1*$^{+/+}$ control FLC mice were sensitized by skin painting with FITC (dissolved in vehicle) or vehicle alone. On day 6 after sensitization, the right and left ears of mice were painted with FITC and vehicle alone, respectively. 24h after elicitation, the thickness of both ears was measured in sensitized and non-sensitized animals. *Left*, absolute change in ear thickness (ΔT in mm x10^{-2}) and percent increase (% values above bars) in FITC and vehicle treated ears. *Right*, Normalized increase in ear thickness calculated as ΔT (FITC treated ear) - ΔT (vehicle treated ear) from data shown in left panel. Bar graphs represent averages (±SEM) from nonsensitized *Orai1*$^{KI/KI}$ mice (n=4), sensitized *Orai1*$^{KI/KI}$ mice (n=7), nonsensitized *Orai1*$^{+/+}$ mice (n=9) and sensitized *Orai1*$^{+/+}$ mice (n=9). p-values, Student's t-test.

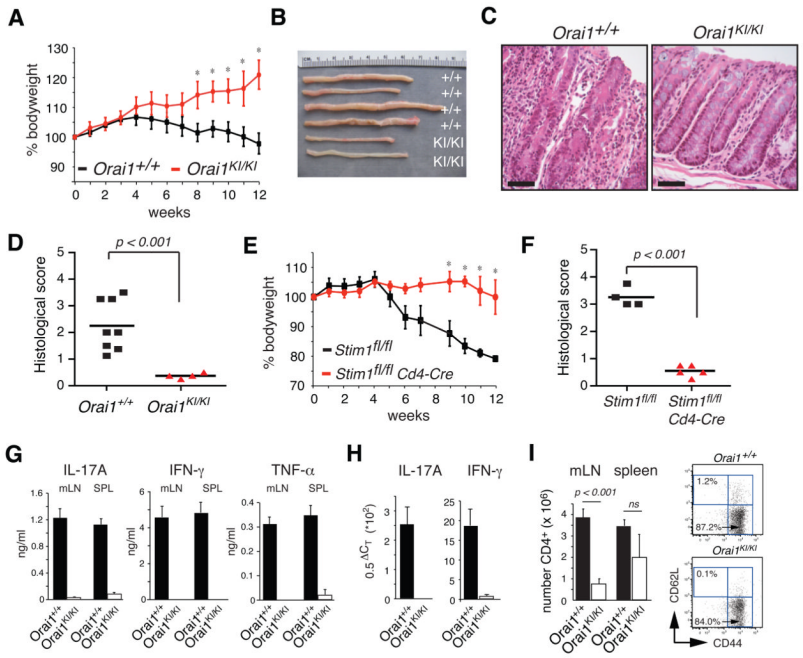

Fig. 6. Naive CD4$^+$ CD45RB$^+$ T cells from *Orai1*$^{KI/KI}$ mice fail to induce colitis

CD4$^+$ CD45RB$^+$ CD25$^-$ T cells from *Orai1*$^{+/+}$ and *Orai1*$^{KI/KI}$ chimeric mice (A–D, G–I) or *Stim1*$^{fl/fl}$ and *Stim1*$^{fl/fl}$ *Cd4-Cre* mice (E–F) were injected into *Rag2*$^{-/-}$ mice to induce colitis. **A**, Body weight in percent of original weight at the time of adoptive T cell transfer. *, $p < 0.05$. **B–C**, 12 weeks after adoptive T cell transfer, colitis is apparent in mice transferred *Orai1*$^{+/+}$ but not *Orai1*$^{KI/KI}$ T cells by increased colon length and diameter (B) and histological signs of colitis (C). A representative example of normal colon lamina propria in *Rag2*$^{-/-}$ mice that had received *Orai1*$^{KI/KI}$ T cells (C, right), and epithelial hyperplasia, loss of goblet cells and inflammation in mice that had received *Orai1*$^{+/+}$ T cells (C, left). Scale bars, 500 μm. **D**, Averaged histological colitis scores (grade 0, no changes; grade 5, severe colitis) from *Rag2*$^{-/-}$ mice adoptively transferred *Orai1*$^{+/+}$ (n=8) and *Orai1*$^{KI/KI}$ (n=4) T cells. Each symbol represents one mouse. **E–F**, Body weight (E) and averaged histological colitis scores (F) from *Rag2*$^{-/-}$ mice adoptively transferred CD4$^+$ CD45RB$^+$ CD25$^-$ T cells from *Stim1*$^{fl/fl}$ (n=4) and *Stim1*$^{fl/fl}$ *Cd4-Cre* (n=5) mice. *, $p < 0.05$ (E). Each symbol represents one mouse. **G–I**, 12 weeks after adoptive T cell transfer, cytokine levels and cell numbers were analyzed in mesenteric lymph nodes (mLN), spleen and colon of mice. **G**, Impaired IL-17A, IFN-γ and TNF-α protein expression by *Orai1*$^{KI/KI}$ CD4$^+$ T cells that were isolated from mesenteric lymph nodes of recipient mice and stimulated *in vitro* for 48h with anti-CD3. Cell culture supernatants were analyzed by ELISA. Averages (±SEM) shown are from 4 *Orai1*$^{+/+}$ and 4 *Orai1*$^{KI/KI}$ T cell transferred mice and two repeat ELISA experiments performed in duplicates. **H**, Severely reduced IFN-γ and IL-17A mRNA expression in colon explants from *Orai1*$^{KI/KI}$ T cell transferred mice compared to *Orai1*$^{+/+}$ control mice. Average (±SEM) cytokine expression in colons of 4 *Orai1*$^{+/+}$ and 2 *Orai1*$^{KI/KI}$ T cell transferred mice from two repeat real-time PCR experiments performed in triplicate. ΔC_T, threshhold cycle differential. **I**, Significantly reduced number of *Orai1*$^{KI/KI}$ CD4$^+$ T cells compared to wildtype T cells in mesenteric lymph nodes of *Rag2*$^{-/-}$ mice (left). Error bars, SEM. p-values, Student's t-test. CD4$^+$ T cells isolated from mesenteric lymph nodes of *Orai1*$^{KI/KI}$ and *Orai1*$^{+/+}$ transferred mice have an activated CD44$^+$ CD62L$^-$ memory phenotype (right).

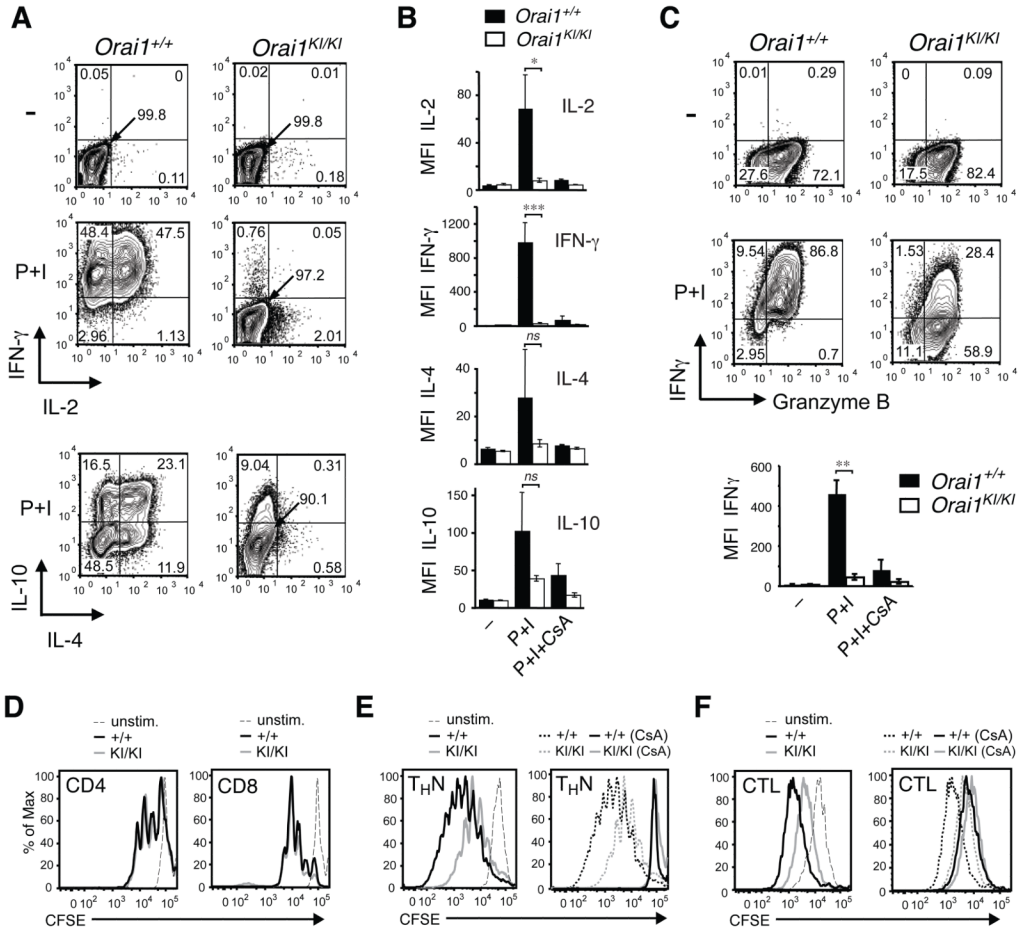

Fig. 7. Impaired effector function of *Orai1*$^{KI/KI}$ T cells *in vitro*

A–C, Severely impaired cytokine production in CD4$^+$ and CD8$^+$ T cells from *Orai1*$^{KI/KI}$ mice. Expression of the indicated cytokines was measured in CD4$^+$ (**A, B**) and CD8$^+$ (**C**) T cells from *Orai1*$^{KI/KI}$ and *Orai1*$^{+/+}$ control mice. T cells were differentiated *in vitro* under non-polarizing conditions in the presence of 20 U/ml (**A, B**) and 100 U/ml (**C**) IL-2. On day 6, cells were left untreated (–) or restimulated for 6 hours with PMA (P) and ionomycin (I) either in the presence or absence of cyclosporin A (CsA). One representative experiment is shown. Bar graphs in B and C represent averages (±SEM) of mean fluorescence intensity (MFI) of cytokine expression from n=4–8 (IL-2, IFN-γ in B), n=3 (IL-4, IL-10 in B) and n=3 (IFN-γ in C) repeat experiments. *, p<0.05; **, p<0.005; ***, p<0.001; ns, not significant. **D–F**, Normal to moderately impaired proliferation of naïve and *in vitro* differentiated T cells from *Orai1*$^{KI/KI}$ mice. **D**, CD4$^+$ and CD8$^+$ T cells were isolated from lymph nodes of *Orai1*$^{KI/KI}$ (gray) and *Orai1*$^{+/+}$ control (black) mice, loaded with CFSE and stimulated with anti-CD3 and anti-CD28 for 3 days. **E–F**, CD4$^+$ and CD8$^+$ T cells from *Orai1*$^{KI/KI}$ (gray) and *Orai1*$^{+/+}$ control (black) mice were differentiated into T_HN cells and cytotoxic T lymphocytes (CTL), respectively, for 3 days in the presence of IL-2, loaded with CFSE and restimulated with anti-CD3 and anti-CD28 for another 3 days without IL-2, either in the presence or absence of cyclosporin A (CsA). Solid lines in right panels of E, F show proliferation of cells in the presence of CsA; proliferation in the absence of CsA (same date as in left panels in E, F) is indicated by dashed lines for comparison. One representative experiment of 3 is shown.

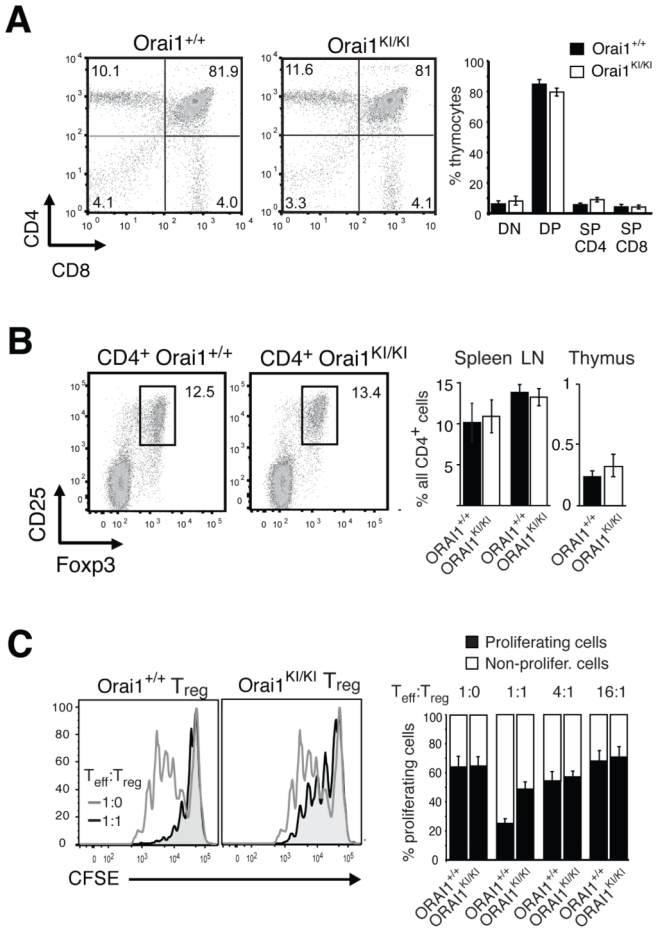

Fig. 8. Normal T cell development but impaired function of T_{reg} cells in *Orai1*$^{KI/KI}$ mice

A, Normal thymic T cell development in *Orai1*$^{KI/KI}$ mice. Thymocytes were isolated from *Orai1*$^{KI/KI}$ and wildtype *Orai1*$^{+/+}$ chimeric mice 5–6 weeks after transfer of fetal liver cells to *Rag2*$^{-/-}$, *cγ* $^{-/-}$ mice and analyzed by flow cytometry. Shown is one representative experiment of 7 (left) and averages (±SEM) of thymocyte populations from *Orai1*$^{KI/KI}$ (n=7) and *Orai1*$^{+/+}$ (n=7) mice. DN, $CD4^{-}CD8^{-}$ double negative; DP, $CD4^{+}CD8^{+}$ double positive; SP, single positive. **B**, Normal numbers of $CD4^{+}$ $CD25^{-}$ $Foxp3^{+}$ regulatory T cells (T_{reg}) cells in lymphoid organs of *Orai1*$^{KI/KI}$ mice. T cells were isolated from thymus, spleen and lymph nodes of *Orai1*$^{KI/KI}$ and *Orai1*$^{+/+}$ wildtype mice and stained with antibodies to CD4, CD25 and Foxp3. One representative experiment of 3 is shown representing splenocytes (left). Percentages of $CD4^{+}$ $CD25^{+}$ $Foxp3^{+}$ T_{reg} cells were comparable in lymph nodes, spleen and thymus of *Orai1*$^{KI/KI}$ and *Orai1*$^{+/+}$ control mice (right). Error bars, SEM. **C**, Impaired suppression by T_{reg} cells from *Orai1*$^{KI/KI}$ mice *in vitro*. CFSE-labeled responder $CD4^{+}$ T cells isolated from wildtype C57BL/6 mice were cocultured with $CD4^{+}$ $CD25^{+}$ T cells (T_{reg}) purified from *Orai1*$^{+/+}$ and *Orai1*$^{KI/KI}$ mice. Cells were incubated for 72h at a 1:1 ratio in the presence of mitomycin C-treated T-cell depleted splenocytes and 0.3 μg/ml anti-CD3 antibodies. Open histograms in left panels: $CD4^{+}$ responder cells alone; shaded histograms: $CD4^{+}$ responder cells co-cultured with wildtype *Orai1*$^{+/+}$ or *Orai1*$^{KI/KI}$ T_{reg} cells. Bar graphs on right show average numbers (±SEM) of dividing (1–6 cell divisions, black) and non-dividing (white) $CD4^{+}$ responder cells incubated with *Orai1*$^{+/+}$ and *Orai1*$^{KI/KI}$ T_{reg} cells at 1:0, 1:1, 4:1 and 16:1 ratios from two independent experiments.